The Music of Rivers: the Mathematics of Waves Reveals Global Structure and Drivers of Streamflow Regime

Brian C. Brown[1,2], Aimee H. Fulerton[3], Darin Kopp[4], Flavia Tromboni[5,6], Arial J. Shogren[7,8], J. Angus Webb[9], Claire Ruffing[10], Matthew Heaton[11], Lenka Kuglerová[12], Daniel C. Allen[13], Lillian McGill[14], Jay P. Zarnetske[15], Matt R. Whiles[16], Jeremy B. Jones Jr.[17], Benjamin W. Abbott[1]

[1]Department of Plant and Wildlife Sciences, Brigham Young University, Provo, Utah, USA.

[2]Department of Computer Science, Brigham Young University, Provo, Utah, USA.

[3]Fish Ecology Division, Northwest Fisheries Science Center, National Marine Fisheries Service, National Oceanic and Atmospheric Administration, Seattle, Washington, USA.

[4]Oak Ridge Institute for Science and Education (ORISE), Corvallis, Oregon, USA.

[5]Global Water Center and Department of Biology, University of Nevada, Reno, Nevada, USA.

[6]Leibniz Institute of Freshwater Ecology and Inland Fisheries, Berlin, Germany.

[7]Earth and Environmental Sciences Department, Michigan State University, East Lansing, Michigan, USA.

[8]Department. of Biological Sciences, University of Alabama, Tuscaloosa Alabama, USA.

[9]Water, Environment and Agriculture Program, Department of Infrastructure Engineering, The University of Melbourne, Victoria, Australia.

[10]The Nature Conservancy in Oregon, Portland, Oregon, USA.

[11]Department of Statistics, Brigham Young University, Provo, Utah, USA.

[12]Department of Forest Ecology and Management, Swedish University of Agricultural Sciences, Umeå, Sweden.

[13]Department of Biology, University of Oklahoma, Norman, Oklahoma, USA.

[14]Center for Quantitative Science, University of Washington, Seattle, Washington, USA.

[15]Department of Earth and Environmental Sciences, Michigan State University, East Lansing, Michigan, USA.

[16]Soil and Water Sciences Department, University of Florida, Gainesville, Florida, USA.

[17]Institute for Arctic Biology, University of Alaska Fairbanks, Fairbanks, Alaska, USA.

Corresponding author: Brian Brown (bcbrown365@gmail.com)

Key Points:

- As complex ecosystem timeseries become longer, we need mathematical tools to understand their structure and links with other parameters.
- Wavelet analyses are tools that can describe complex timeseries such as streamflow, providing a complement to traditional flow metrics.

- A global wavelet analysis of streamflow reveals that variability at short timescales is negatively correlated with long timescales.

Abstract

River flows change on timescales ranging from minutes to millennia. These variations influence fundamental functions of ecosystems, including biogeochemical fluxes, aquatic habitat, and human society. Efforts to describe temporal variation in river flow—i.e., flow regime—have resulted in hundreds of unique descriptors, complicating interpretation and identification of global drivers of flow dynamics. Here, we used a cross-disciplinary analytical approach to investigate two related questions: 1. Is there a low-dimensional structure that can be used to simplify descriptions of streamflow regime? 2. What catchment characteristics are most associated with that structure? Using a global database of daily river discharge from 1988-2016 for 3,120 stations, we calculated 189 traditional flow metrics, which we compared to the results of a wavelet analysis. Both quantification techniques independently revealed that streamflow data contain substantial low-dimensional structure that correlates closely with a small number of catchment characteristics. This structure provides a framework for understanding fundamental controls of river flow variability across multiple timescales. Climate was the most important variable across all timescales, especially those lasting several weeks, and likely contributes as much as dams in controlling flow regime. Catchment area was critical for timescales lasting several days, as was human impact for timescales lasting several years. In addition, both methods suggested that streamflow data also contain high-dimensional structure that is harder to predict from a small number of catchment characteristics (i.e. is dependent on land use, soil structure, etc.), and which accounts for the difficulty of producing simple hydrological models that generalize well.

1 Introduction

River flow drives the structure and function of aquatic systems on sub-daily to decadal timescales, and sculpts landscapes on geological timescales from centuries to millennia (Fisher et al., 1998; Pinay et al., 2018; Tucker & Hancock, 2010). For people, variability in river flow regulates access to freshwater, with extreme flow events such as floods and droughts imposing immense personal and societal costs (Abbott, Bishop, Zarnetske, Minaudo, et al., 2019; Van Loon et al., 2016; Vörösmarty et al., 2010). For ecosystems, water flow through soils, aquifers, and surface-water networks mediates aquatic and riparian biodiversity (Bochet et al., 2020; Hain et al., 2018; N. LeRoy Poff et al., 1997; N. Leroy Poff & Zimmerman, 2010). Additionally, the direction, volume, and timing of flow define terrestrial-aquatic connectivity, and thereby mediate the delivery of biogeochemical substituents, including pollutants, to aquatic and marine ecosystems, including human pathogens, excess nutrients, and novel entities (Raymond et al., 2016; Bernhardt et al., 2017; Moatar et al., 2017; Zarnetske et al., 2018; Frei et al., 2020; Gorski & Zimmer, 2021; S. Liu et al., 2022). From the various viewpoints of human society, biogeochemical fluxes, and aquatic habitat, no single timescale stands out as singularly important regarding flow regime (Fig. 1).

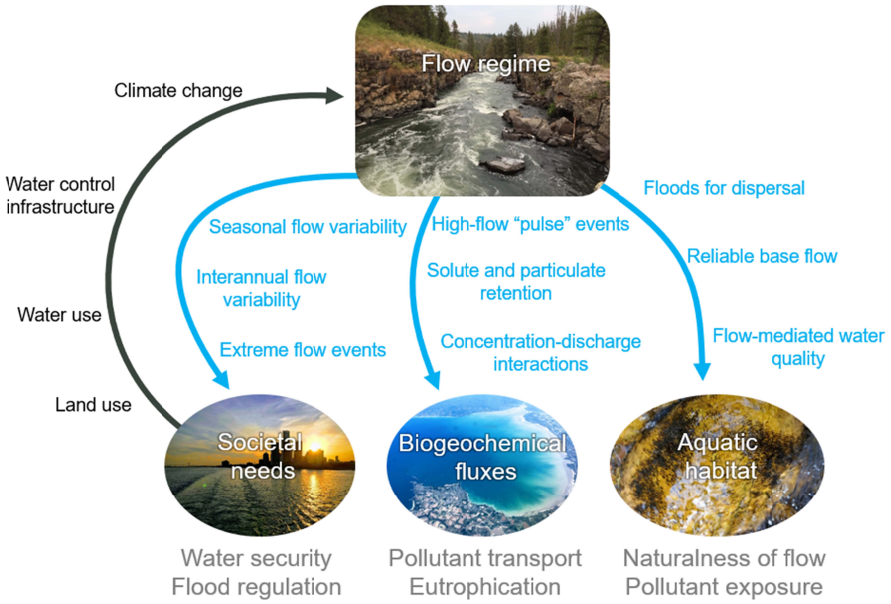

Figure 1. Conceptual diagram representing the societal, biogeochemical, and ecological importance of river flow regime. The relevant dimensions of flow regime are represented in blue, the consequences of flow regime are in gray, and the human influences on flow regime are in black.

In the Anthropocene, human interference with climate, land, and water is threatening aquatic ecosystems, human water security, and biogeochemical cycles at planetary scales (Abbott, Bishop, Zarnetske, Hannah, et al., 2019; Döll & Schmied, 2012; Gleeson et al., 2020; Hogeboom et al., 2020; Lin et al., 2019; Zipper et al., 2020). This creates a pressing scientific challenge and opportunity to identify how climate and catchment parameters interact with direct human modifications of rivers such as dams and levees to influence river flow, and in turn shape the hydrological resilience of socioecological communities (Abbott et al., 2018; Berghuijs et al., 2019; Bunn & Arthington, 2002; Díaz et al., 2019; Harrison et al., 2018; Teixeira et al., 2019). As human modification of land, water, and the atmosphere increase (Ascott et al., 2021; Minaudo et al., 2017; Zhou et al., 2015), understanding how to describe and predict river flow in the context of human involvement is becoming increasingly important.

Though global datasets of river flow observations and modeled natural discharge rates are now available (Alfieri et al., 2020; Gerten et al., 2008; Hales et al., n.d.; Hannah et al., 2011; J. Liu et al., 2018; Masaki et al., 2017; McMahon et al., 2007), a unified framework for describing and interpreting river flow across multiple relevant timescales has not been widely adopted (McMillan, 2021). Efforts to quantify flow regime (e.g. variation in river discharge, including magnitude, frequency, duration, timing, and rate of change of flow) have resulted in the development of over 600 metrics (George et al., 2021; Gnann et al., 2021; Jones et al., 2014; N. LeRoy Poff et al., 1997). Many of these metrics are designed to describe key features of flow pertinent to society and ecosystems, such as interannual variability of low flows and the seasonal timing of flooding. Other metrics are designed to quantify hydrological processes such as the rate of increase and decrease of flow following rain, or baseflow conditions between storm events (Archfield et al., 2014; Carlisle et al., 2010; McMillan, 2021). While all these metrics are useful

for individual studies and management, their sheer range and redundancy creates a problem of comparability at regional to global scales (Olden & Poff, 2003). In addition to these "traditional" flow metrics, the strictly hydrological literature has widely used the spectral properties of flow regime obtained via wavelet decomposition, an analytical technique which leverages the concise mathematics of waves to describe variability at multiple timescales simultaneously. Wavelet analyses are used to identify which timescales are most important in a timeseries (Carey et al., 2013; Labat, 2010; Sang, 2013; Smith et al., 1998; White et al., 2005). Wavelet decompositions and the traditional flow metrics are rarely used in concert, and similarities and differences between the two approaches have not been quantified.

The complexity of measuring and characterizing flow regime likely contributes to the persistent difficulty in understanding the factors influencing river flow. Even when constraining the discussion to specific timescales or metrics such as annual flow or runoff ratios during storm events, the physical, biological, and human controls on flow at the catchment scale are still being debated (Lane et al., 2017; Lin et al., 2019; Reaver et al., 2020; Savenije, 2018; Sivapalan, 2006; Tetzlaff et al., 2008; Zhou et al., 2015). Climatic, surface, and subsurface parameters have been proposed as primary controls on the timing and magnitude of river flow across sites, including the amount of soil and aquifer water storage, the relative availability of energy and water, the configuration and size of the surface water network, and the extent and type of vegetation (Carlisle et al., 2010; Lane et al., 2017; Oldfield, 2016; Ryo et al., 2015; Sanborn & Bledsoe, 2006; Zhou et al., 2015). Regardless of the method, understanding variation and similarity in flow regimes across biomes and ecoregions could reveal drivers of aquatic ecology and explain differences in success of water management and ecosystem protections in different conditions (Berghuijs et al., 2019; Bunn & Arthington, 2002; Zhou et al., 2015).

In this context, we analyzed a global dataset of river flow to compare methods for characterizing flow regime and to identify flow relationships with climatic and catchment factors. We combined traditional flow metrics with wavelet analysis to describe 3,120 time series of river flow, each with over 9 years of continuous data between 1988 and 2016. In addition to quantifying the relationship between streamflow metrics and wavelet analysis, we sought to identify which climatic, geomorphological, and human attributes are most important for determining variability in flow at timescales ranging from days to a decade. These flow behaviors across timescales are rarely analyzed in concert (McMillan, 2021; Olden & Poff, 2003), but we further hypothesized that variability in flow at different timescales acts as an interacting set of variables, meaning that changes in flow volume that last only a few days are fundamentally linked to changes in flow volume that last several years. If present, these linkages would imply low-dimensional structure in streamflow data, which we believe would be fundamental to developing a concise vocabulary for describing streamflow regime and understanding its controls. Because the same climatic and catchment attributes influence flow on multiple timescales, considering potential interactions across timescales could open new pathways towards understanding and predicting flow regimes. For example, because the relative abundance of energy and water influence vegetation and soil development (Malone et al., 2018; Tank et al., 2020), hot and dry catchments could simultaneously exhibit high seasonal variability in flow and greater extractive human water use, causing long-term reductions in the water table. Likewise, because larger catchments integrate heterogenous subcatchments over larger and longer spatiotemporal scales (Chezik et al., 2017; Dupas et al., 2019; Levia et al., 2020), we predict they will show less short-term variability but greater sensitivity to long-term changes in water balance.

2 Materials and Methods

2.1 River flow and catchment characteristics data

We obtained daily river discharge time series from the Global Runoff Data Centre (GRDC; https://www.bafg.de/GRDC). We used several criteria to select from the 6,544 stations with discharge data from a recent 30-year period of interest (1988-2016). Because continuous time series are required for the calculation of many flow metrics, we first removed stations that had less than nine complete water years over the period of interest. This left us with 4,762 candidate stations (2,399 without any gaps and 2,363 with some gaps). For all stations, we removed records for partial water years, i.e., those before the first complete water year or after the last complete water year. For those time series with gaps, we computed the number of days in each missing period and the total number of missing periods. We summarized the number of missing days (e.g., minimum, mean, maximum, and percentiles), and calculated the proportion of days in the record for which data were available. We filled gaps via linear interpolation for stations that met the following criteria: $\leq$ 25% missing data, the longest data gap was less than 2 years, and the 75th percentile of consecutive days of missing data was less than 3 months. For stations that passed this test (1,163 of the 2,363), we visually inspected the result of interpolation to ensure that obvious peaks or troughs in each station's data record were not omitted. We discarded 104 stations that showed anomalous effects during interpolation, leaving 1,059 stations. For the stations with gaps that did not meet our criteria, 509 were located more than 1 km from an included station, and many were in data-sparse regions with relatively few observations. Despite their gaps, some of these stations had long data records within the period of interest. Therefore, we determined which stations had sufficiently long ($\geq$9 y) intact stretches that could be extracted from the longer time series. We were able to salvage an additional 227 stations using an automated approach followed by visual inspection. Therefore, our final set of stations included those with complete records (2,399), those with interpolation that met our inclusion criteria (1,059), and additional salvaged stations (227), for a total of 3,685 stations—56% of the original GRDC stations.

The GRDC streamflow dataset reports the upstream catchment area associated with each station but does not directly reference them to the hydrography we used in this study. As such, differences in data sources could have created mismatches between the location of a GRDC station and the upstream catchment we delineated from the integrated Shuttle Radar Topography Mission (SRTM) digital elevation model and the GTOPO30 Digital Elevation Model (DEM, http://files.ntsg.umt.edu/data/DRT). Following Barbarossa et al. (2018), we geo-referenced each station to the pixel that was most similar in catchment area and within 5 km from its original location. We designated stations as high, medium, or low quality if the difference in catchment area was <5%, 5% to 10%, or 10% to 50%, respectively (Barbarossa et al., 2018).

After delineating each watershed, we extracted 117 variables obtained from a variety of geospatial data sources (supplemental table S1). These variables capture the stream network structure, climate, landcover (including lakes and soils), and anthropogenic impacts (including population density and reservoirs) upstream of each GRDC location. Depending on the parameter, we calculated cumulative values (e.g., total precipitation) or catchment means (e.g., mean annual temperature). Because the configuration and density of stream networks can influence propagation of water and solutes (Godsey & Kirchner, 2014; Helton et al., 2011), we quantified stream network structure using TauDem (Terrain Analysis Using Digital Elevation Models, https://hydrology.usu.edu/taudem/taudem5/). This open-source software implements

highly parallelized algorithms that can efficiently process large datasets (Barbarossa et al., 2018). We used the AreaD8 function to calculate the number of pixels upslope from a station (i.e., the flow accumulation grid) and the GridNet function to calculate stream network attributes (e.g., stream order and total network length). In addition to comparing catchment attributes with flow regime metrics, we calculated pairwise correlations between catchment characteristics to test for collinearity. Because of missing geospatial data, as few as 3,120 streams were used in these analyses.

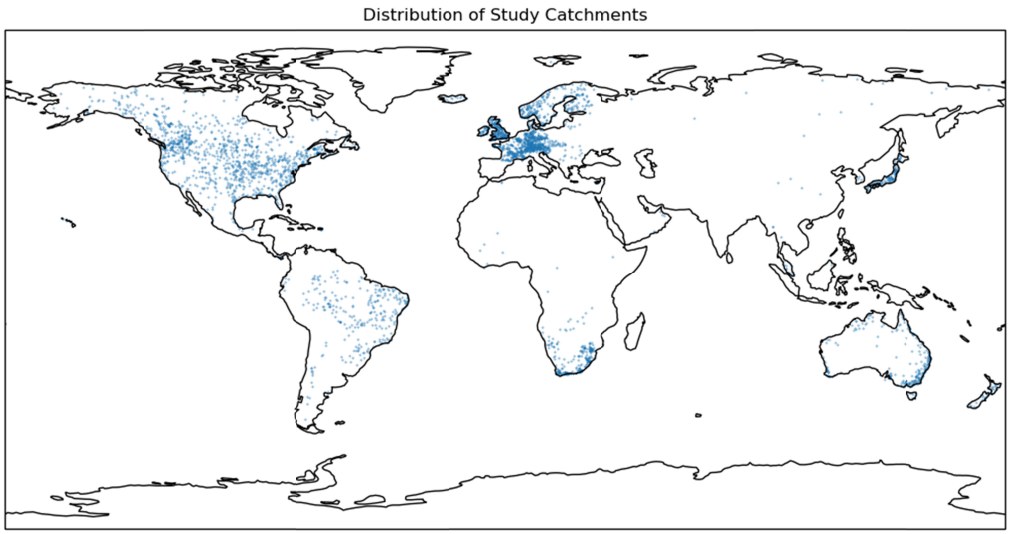

Figure 2. Distribution of catchments used in this study. Each dot represents a flow gage with nine or more years of daily flow data during the study period and minimal gaps.

2.2 Characterizing flow regime – conceptual introductions

Frequency decompositions rely on the fact that timeseries are fundamentally related to waves. Waves are phenomena that repeat through time, and can occur in any number of dimensions, though in this scope we consider one-dimensional waves that represent a single variable changing through time. Waves can be described with five fundamental descriptors: (1) *amplitude*: magnitude of variation around the mean, or equilibrium point; (2) *phase*: horizontal shift or timing of the oscillation; (3) *vertical shift*: changes in the level of the mean; (4) *waveform*: differences in the shape of the repeating pattern (e.g., a typical sinusoid curve, or a more unusual shape such as a square, triangle, or saw-tooth shape); and (5) *frequency*: the number of oscillations that occur within a given timeframe. Together, amplitude, phase, vertical shift, waveform, and frequency describe essentially any difference between any two waves (figure 3).

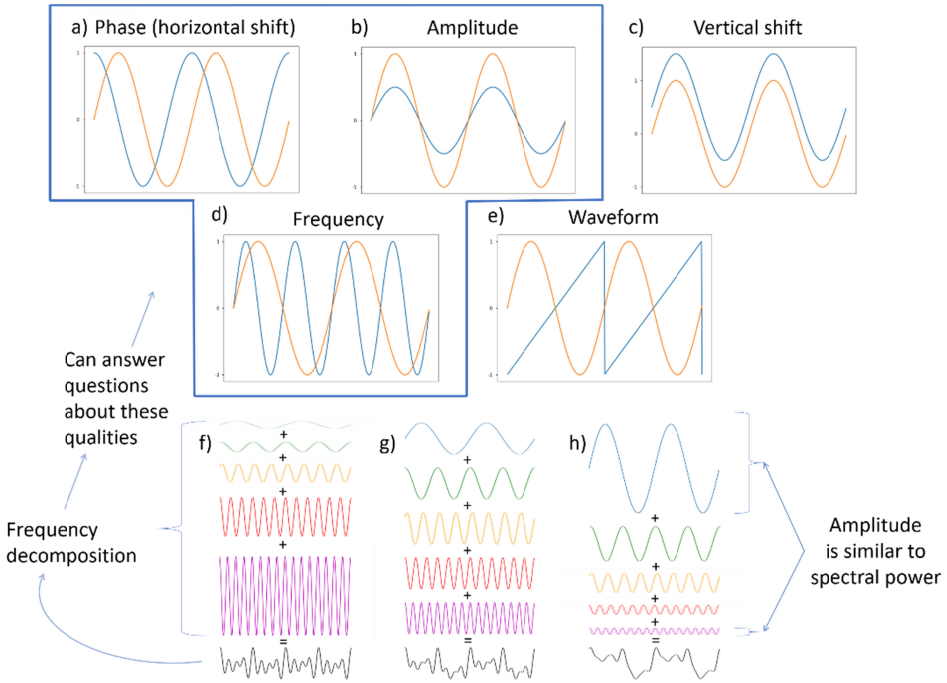

Figure 3. (a – e) Five fundamental components of flow regime (or any time series): Many of the behaviors in streamflow timeseries relate back to these five fundamental principles. The lower portion of the figure represents frequency decompositions of three timeseries: f) a timeseries dominated by high-frequency variability, g) a timeseries with equal variability across all timescales, and h) a timeseries dominated by low-frequency variability. In each example, adding together the five colored waves produces the complex curve shown in black at the bottom.

The terms phase, amplitude, vertical shift, frequency, and waveform have familiar analogues in hydrology. Consider an imaginary catchment with a hydrograph that follows a perfect sinusoidal curve that goes up and down over the course of a year. The amplitude of this wave plus any vertical shift relates closely to the familiar concept of peak annual flow, and vertical shift minus the amplitude relates to baseflow, or minimum flow. In this catchment, the frequency of one cycle per *year* relates to the timescale containing the most variance. The phase of the wave indicates the time of year snowmelt or monsoon rains occur, and would be opposite for a northern vs southern hemisphere catchment. The waveform relates to the rate of rise or fall of the year-long increase and decrease in flow. Now imagine a second catchment whose flow follows another perfect sinusoidal wave, but which oscillates at one cycle per two weeks. This "flashy" catchment neither accrues nor loses long-term storage, and might hypothetically occur in a warm climate with no snow but with identical rain storms every two weeks. Both catchments exhibit variability in flow, but in the first, the variance is maximized at the timescale of one year, and in the second at two weeks.

However, most catchments exhibit both flashiness and some seasonal variability. Adding together the perfect sine wave from the first catchment with the perfect sine wave from the second catchment would produce a complex curve that can no longer be described with amplitude, phase, vertical shift, waveform, and frequency, but which more closely resembles a real-world catchment. This process of adding new catchments that epitomize behavior on different timescales could be repeated infinitely many times, producing an ever more complex, and hence more realistic hydrograph, but which could always be decomposed back into a collection of simple waves that can individually be described by the same few, succinct

variables. Mathematical tools exist to run this process *backwards*—decomposing a timeseries into a set of perfect sinusoids that together recreate the original timeseries. These are known as *frequency decompositions,* and can be thought of as functioning similarly to a prism, which decomposes white light into a rainbow of colors ranging from high to low frequency, or to a computer program that takes in the sound recording of a symphony and outputs a musical score of notes representing air vibrations at particular frequencies. No matter the timeseries, the amplitudes of the resultant decomposed waves at different frequencies relate to the amount of variability in the data that occurs on those timescales, reported in a characteristic known as *spectral power*. Spectral power thus provides a unit for describing variability in streamflow across every timescale present in a hydrograph.

Decision trees are a primal machine learning model that are foundational to many more complex models, such as random forests and gradient boosting forests. Conceptually, decision trees take in an array of prediction features and step-by-step combine multiple points of data along the feature array. Using relatively simple logic, they distill information further and further until a single prediction is made (Myles et al., 2004). Decision trees are generally known to have high bias (typically viewed as undesirable) with low variance, though they are still occasionally used because of their inherent interpretability.

Random forests are called "forests" because they comprise many individual decision trees, usually of significant depth, whose collective predictions are averaged to produce an output that is generally less biased and more accurate than individual decision tree regressors (Biau & Scornet, 2016). The "random" aspect comes from an innovation in 2001 where successive trees are trained on independent random samples with replacement from the larger dataset (Breiman, 2001).

Gradient boosting regressors are similar to random forest regressors, but they differ in that new trees are added in a way that minimizes error in a targeted, rather than a random fashion. This targeted approach is achieved by adding new trees according to the gradient of a user-defined loss function, which is simply a function which characterizes the error of the model (Elith et al., 2008).

Principal Components Analysis, or *PCA,* projects high dimensional data onto a lower dimensional space where each axis is a linear combination of the original variables in the high dimensional space, and where the number of dimensions projected onto is the user's choice. As an intuitive example, imagine a "high-dimensional" dataset with two variables, x and y. If, for every step in the x direction, data tend to take two steps in the y direction, the two variables are redundant and linearly related; total least squares linear regression would draw a line through the two axes with a slope of ~2. PCA on these two axes would project data points onto that regression line. That is, instead of listing data points by their x and y coordinates, the PCA projection would list data points by their location on a new axis, z, which is two parts y, and one part x. The "two parts" and "one part" that describe how much each original axis contributes to the new projected axis are referred to as the *loadings matrix.* The loadings matrix effectively describes how correlated (positive or negative) each of the original axes in the high-dimensional space is with the low-dimensional axes PCA projects the data onto. Thus, like wavelet decompositions, PCA identifies variability in data. But instead of identifying variability at different timescales in a timeseries, PCA identifies variables (or combination of variables) in tabular data along which the data vary most. If a group of original variables (columns) have high magnitude loadings for a given principal component, then that principal component can be thought of as a combination of those original variables. In other words, the resulting components

from PCA describe low-dimensional linear structure in data which in turn corresponds to simple, high-level concepts. Examining the loadings matrix is one of the best methods for adding interpretability to the abstract components that result from a PCA projection.

2.3 Streamflow analysis

2.3.1 Quantifying Streamflow Regime

Traditional methods for describing streamflow regime include over 600 flow regime metrics available in the literature that describe concepts such as variability in monthly flow, annual maximum of 90-day moving average of flow, low flood pulse count, etc., and are collectively both diverse and in many cases redundant (Olden and Poff 2003). We calculated a subset of these metrics that are commonly used in hydrology, based on the availability of statistical packages and recent flow regime papers. First, we calculated the "Magnificent 7" (Mag7; Archfield *et al.* 2014). Second, we calculated 171 metrics from the Hydrological Index Tool (HIT; Henriksen *et al.* 2006), reimplemented in the EflowStats package (Archfield et al. 2013). Finally, we calculated the 11 metrics from Sabo and Post (SP; Sabo & Post 2008), for a total of 189 metrics. Given previously identified redundancy in in streamflow metrics (Olden and Poff 2003), we are confident that this set covers the full range of hydrological variability.

To identify the amount of redundancy in the selected metrics we applied PCA using the R package FRK and the NNGP method (Zammit2-Mangion & Cressie, 2017). We retained 7 dimensions for further analysis and which we hereafter refer to as "PCA Metrics." These 7 dimensions collectively explained 68% of the variability in the 189 streamflow metrics. We summarized the top correlates suggested by the loadings matrix (see section 2.2) to provide qualitative descriptors of the resulting metrics. Separately, we quantified streamflow regime using a frequency decomposition. Classically, frequency decompositions are performed using the discrete-time Fourier transform, yielding an output that quantifies the variability in the signal at different timescales using a unit called "spectral power" (Unpingco 2014). Recently it has become more common to use a related analysis called a Wavelet transform (Carey et al., 2013; Labat, 2010; Sang, 2013; Smith et al., 1998; White et al., 2005), which generates a blended time-frequency decomposition of the input. We then averaged spectral power across time to obtain a frequency-only representation of the original signal, after finding that this technique produced distinct peaks at plausible frequencies with minimal noise. We calculated the time-averaged wavelet decomposition using the default settings of the WaveletComp R package (Rösch and Schmidbauer 2018). While several wavelet forms are possible to choose from within the WaveletComp package, we chose the Morlet wavelet, which is considered suitable for many climate-linked timeseries (Torrence & Compo, 1998).

2.3.2 Similarities between streamflow metrics and frequency decomposition

We calculated Spearman correlations between each frequency's spectral power and each of the 189 flow metrics across all catchments in the dataset. Seeking to confirm the results of the correlation analysis through an alternate technique, we also trained machine learning models to predict each of the streamflow metrics using the frequency decompositions as inputs. To account for variability between models and divisions of data, 18 models were trained on each of the 189 streamflow metrics. For each metric, 9 were random forest regressors and 9 were gradient boosting regressors. Data were divided with an 80:20 training to testing ratio, with the divisions

done randomly and independently for each model. Models were then validated on the 20% portion reserved for testing and an r-squared was calculated between model output and the actual values of the given streamflow metric for the 20% testing data. Finally, the "feature importances" were extracted from each model to determine which input features were most important in the models' decision-making processes (Frei et al., 2021). Models were implemented in Python using the Sci-kit Learn library and feature importances were extracted using the "feature_importance_" method (Pedregosa et al., 2011).

To connect the previously-calculated PCA axes to frequency analyses, we ran a Spearman correlation analyses between each of these PCA metrics and the spectral power of each frequency. Similar to each of the 189 flow metrics, we also trained 360 machine learning models, with an even split between random forest regressors and gradient boosting regressor models, to predict each PCA metric using the frequency domain, again with a unique, random 80:20 split between training and testing data.

Structure in the outputs of these three analyses suggested that variability at shorter timescales was linked to variability at longer timescales. To isolate and quantify this phenomenon, we calculated the pairwise spearman rank correlation between the spectral powers at each frequency and the spectral powers at all other frequencies.

2.3.3 Identifying controls on streamflow regime

Whereas in the previous section we sought to quantify similarities between methods for describing streamflow regime, in the following section we describe analyses in which we sought to understand which catchment characteristics are the best predictors (and therefore likely controls) of flow regime. Consequently, we trained three separate machine learning models, a decision tree regressor, a random forest regressor, and a gradient boosting regressor, to predict each of the PCA metrics (which we consider concise surrogates for the full 189 flow metrics we calculated) from the 117 catchment characteristic input features. We used the k-folds validation process with a k of 10, meaning that we trained 10 separate models on different 90:10 splits of data and validated each model on the unique 10% of the data not used for training that model. Validation was done by calculating model r-squared between predictions and ground truth. Prior to training, data were normalized using min/max normalization. As before, feature importances were extracted to understand which input features (i.e. catchment characteristics) were most important in determining flow regime. To confirm these results we also ran a Spearman correlation analysis between the 117 streamflow metrics and the spectral power for each frequency. All correlation analyses in this paper were implemented using the Scipy library in python (Virtanen et al., 2020).

Additionally, we trained three classes of machine learning models to predict the spectral power of streamflow timeseries at different frequencies. Similar to the machine learning analysis predicting streamflow metrics from wavelet analyses, for each of the 1101 frequencies identified by the wavelet analysis, we trained 20 random forest regressors and 20 gradient boosting regressors to predict spectral power using catchment characteristics. We divided data with an 80:20 training to testing ratio, with the divisions done randomly and independently for each model. Models were then validated on the 20% portion reserved for testing and an r-squared was calculated between model output and the actual values of the given streamflow metric for the 20% testing data. Data were normalized to be mean zero and standard deviation of 1. The importance of each prediction feature was then extracted from the models and features were grouped into categories to determine which categories of features were most important for

382 predicting streamflow regime. These results were also confirmed by calculating the Spearman
383 correlation between each of the 117 catchment characteristics and the spectral power for each
384 frequency.

385 **3 Results**

386 3.1 Similarities between streamflow metrics and frequency decompositions

387 Several lines of evidence suggested that streamflow metrics and frequency
388 decompositions carry a substantial amount of similar information. For example, the average
389 maximum Spearman correlation coefficient between the 189 flow metrics and any frequency in
390 the frequency decompositions was 0.46 (supplemental figures S1 and S2). Similarly, the average
391 r-squared for machine learning models trained to predict the 189 flow metrics exclusively using
392 the frequency decomposition was 0.33 (supplemental figures S3 and S4). And finally, the
393 average r-squared for machine learning models that were trained to predict the 7 PCA flow
394 metrics exclusively using the frequency decomposition was 0.42. Together, these results indicate
395 that frequency decompositions such as the wavelet transform describe between 30-45% of the
396 same information as streamflow metrics (or alternatively that both approaches describe
397 phenomena that are highly correlated).

398 3.2 Low-dimensional structure in streamflow timeseries

399 PCA analysis of streamflow metrics suggested that substantial low-dimensional linear
400 structure exists alongside a nontrivial amount of nonlinear structure in streamflow data: 68% of
401 the variance in the original 189 flow metrics could be explained in 7 PCA axes, each capturing
402 increasingly less variability in the data (supplemental figure S5). PCA metrics that explained
403 more variance in the original 189 metrics tended to correlate more strongly to the frequency
404 domain (e.g. metrics 1-4), while those that explained less variance in the original metrics tended
405 to relate less strongly to the frequency domain (e.g. metrics 5-7) (supplemental figure S7). A
406 summary of the loading matrices of each metric are found in Table 1, and more extensive
407 descriptions of the matrices are given in supplemental tables S2-S8. The spatial distributions of
408 the metrics across the globe are plotted in supplemental figure S6.
409

Table 1. List of top seven principal components derived from 189 flow metrics calculated for 3,685 river flow time series.

PCA (%variance explained)	Name	Description of correlates	Hypothesized cause(s)
1, (26%)	Magnitude	High total amount of flow, high minimum flows (rarely dry), and low flow variation in high flows	Big rivers
2, (16%)	High-frequency stability	Long-lasting but infrequent high flows, large portion of flux occurs at high flows, few reversals or short-term changes in direction, few low flow events, red or black noise in the daily discharge data, and strong and skewed seasonal signal.	Big rivers (surface-dominated or unduly influenced by high-flow tributaries)
3, (9%)	Low-frequency stability	High interannual flow stability, low event flashiness, predictable interannual high	High overall storage, low synchrony among sub-

		flows, low flood frequency, high base flow	catchments, groundwater dominated
4, (6%)	Interannual variability	Low interannual stability in high flow magnitude and duration, low stability in annual flow, low seasonality, low annual flow (specific and absolute), variable timing of annual min and max flow, frequent floods, skewed annual flows, variable event response, short-lived flow events	Arid or semi-arid sites
5, (6%)	High and stable baseflow	High baseflow (rarely dry), high skewness, low exceedance flows, frequent floods of moderate magnitude, variable flow, variable moderate flows, variable event response	Near-surface groundwater
6, (3%)	Variable baseflow	Variability in number of no-flow days, very few and short baseflow pulses, high flow constancy and predictability (same timing of variation), more zero-flow months, little range in daily flows, little autocorrelation, higher minimum annual flow, later arrival of minimum flow (freshet pattern), high skewness, more no-flow days	Snowmelt, intermittency, semi-arid, flashy
7, (2%)	Daily variability	High spread in daily flows, low magnitude of interannual high flows, consistently rapid changes in flow, low variability in no-flow days, short and small pulses, more no-flow months, seasonally variable flooding, high signal to noise, variable monthly flows, later arrival of max flows (monsoonal), high interannual variability, frequent floods	Arid, small headwaters, Mediterranean

410

411 Wavelet analysis of streamflow timeseries also suggested that streamflow data are highly
412 compressible (and therefore easily summarized). Spectral power of high frequencies was
413 negatively correlated with spectral power of low frequencies (figure 4). This indicates that a
414 tradeoff exists between changes in flow that occur over several days and changes in flow that
415 occur over several months or years. This structure also indicates that streamflow data are
416 extremely low-dimensional when represented in the frequency domain. Figure 5 demonstrates
417 the tradeoff between long and short-term variability in flow data using example hydrographs and
418 their associated frequency decompositions from our dataset.

419

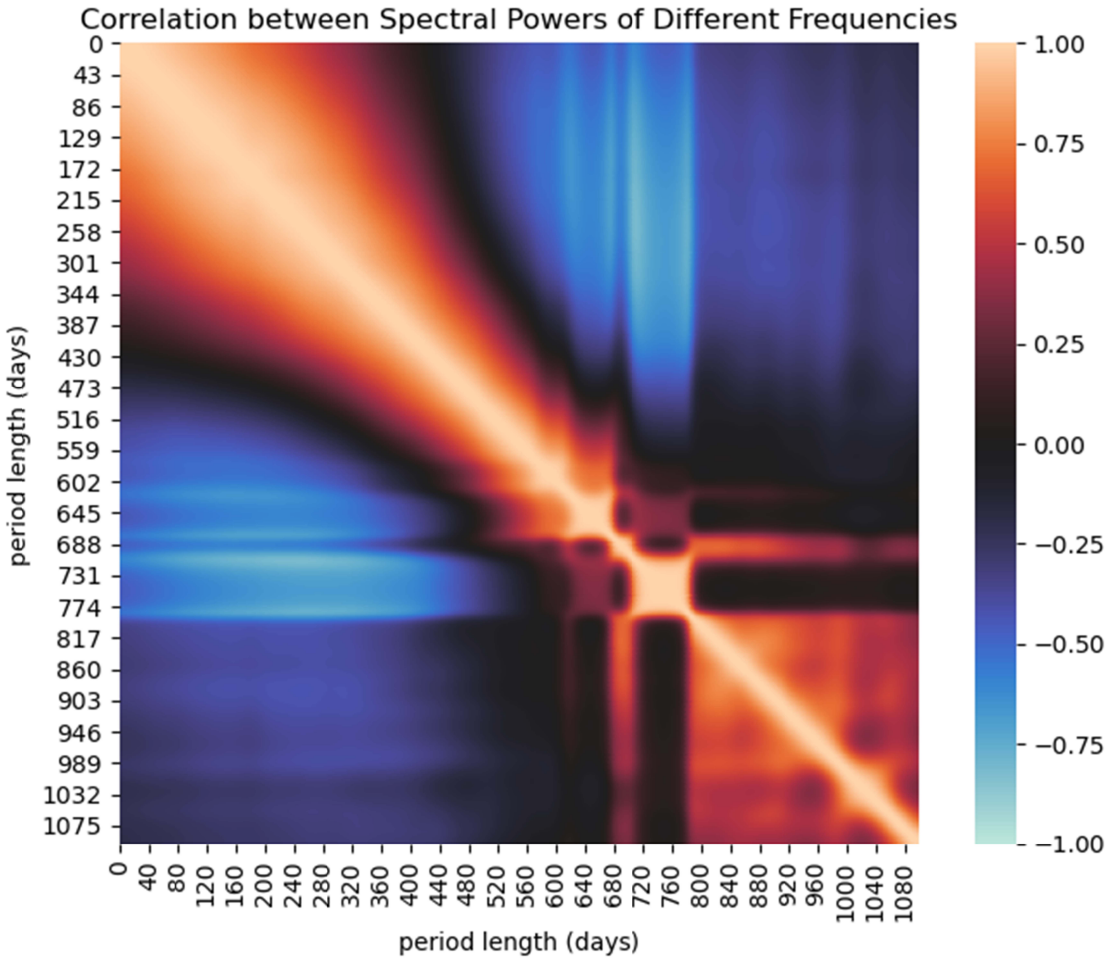

Figure 4. Pairwise correlations between spectral power for each period length. The coefficient of correlation from the spearman correlation is represented as color, with brighter orange representing a stronger positive monotonic relationship and brighter blue representing a stronger negative monotonic relationship. This unexpectedly simple structure in the data suggests that even non-redundant streamflow metrics may be correlated with each other because inherent correlations exist between variability at short timescales and variability at long timescales. The coherent patterns imply that streamflow data are low-dimensional and easily compressed (described). This low-dimensionality also suggests that a relatively small number of mechanisms may govern streamflow variability across multiple timescales.

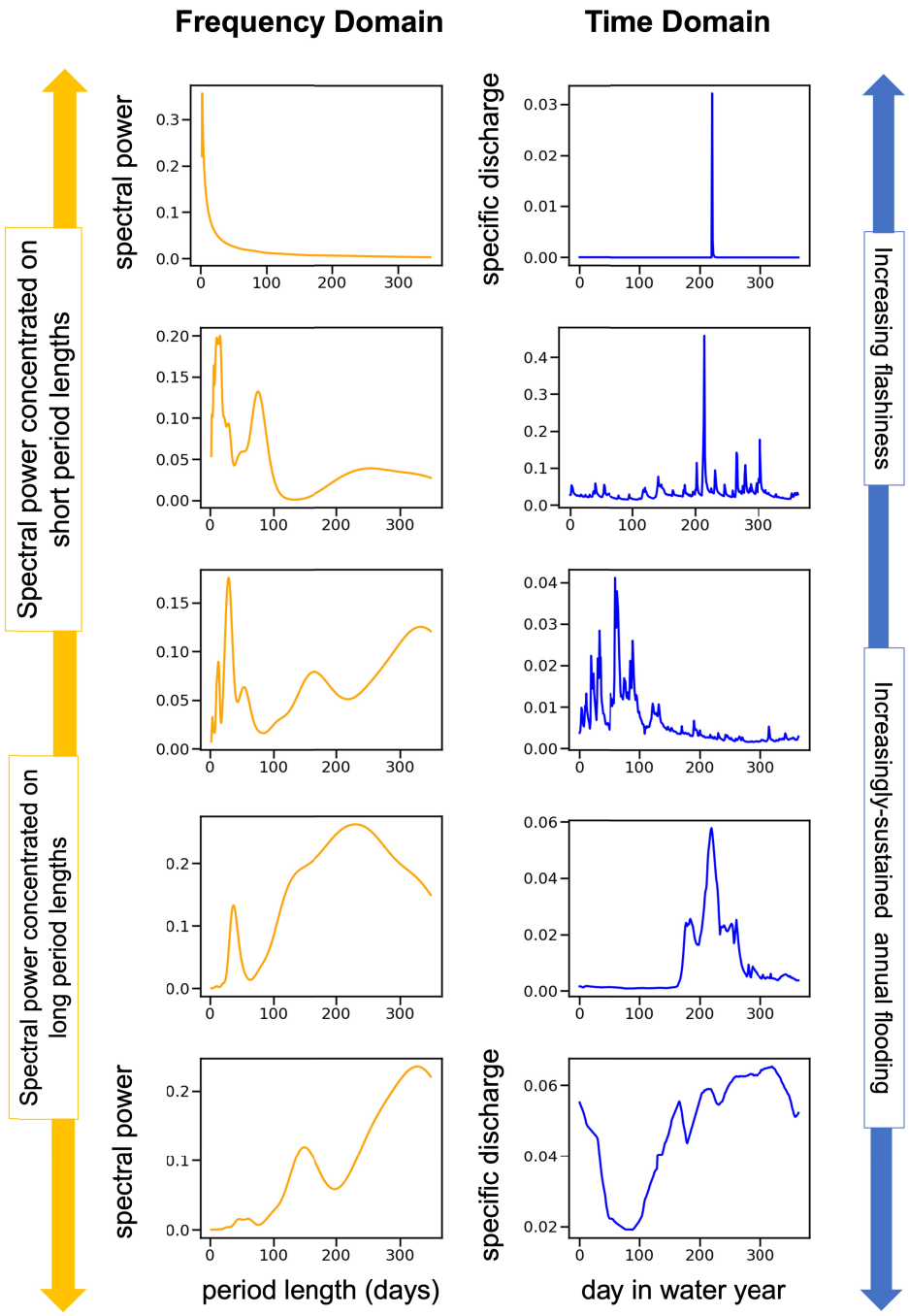

Figure 5. Comparison between frequency domain and time domain representations of hydrographs. Frequency domain representations (pictured on the left in yellow) show how much variability in the data occurs along a particular time scale, while their corresponding time-domain representations (pictured on the right in blue) show the raw time series measured by streamflow gauges. The frequency domain representation allows for the quantification of many qualitative attributes of flow regime properties that might otherwise take dozens of metrics to fully describe. Note that these example hydrographs anecdotally demonstrate the global phenomenon that spectral power at short period lengths is negatively correlated with spectral power at long period lengths.

We also found that on average, variability in flow occurs at four distinct timescales (Figure 6). These are multi-day variations, multi-month variations, annual variations, and multi-annual variations. Annual variation was the strongest, followed by multi-month variation and multi-day.

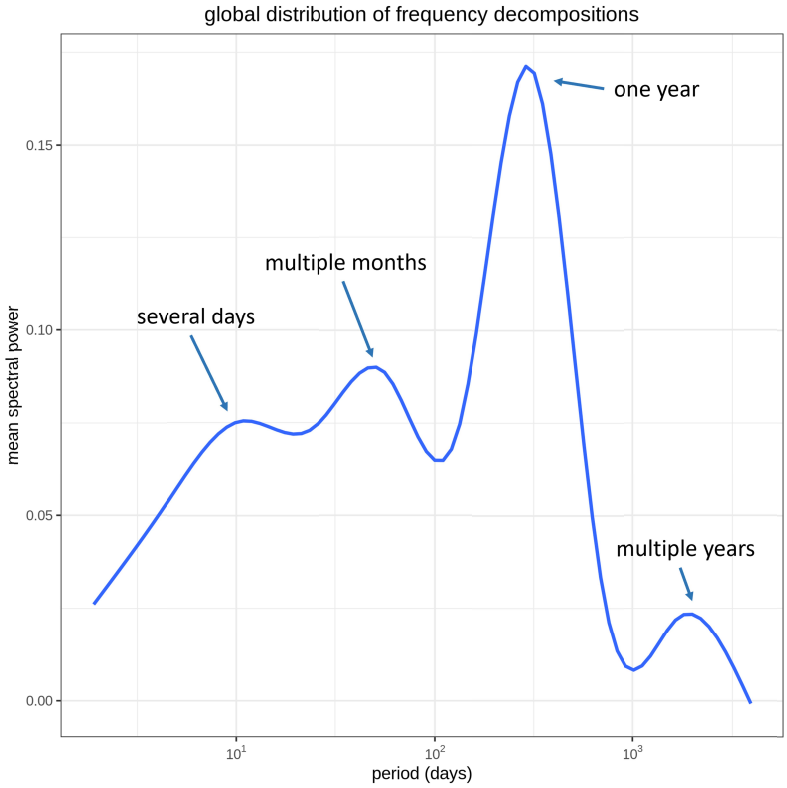

Figure 6. Mean global spectral decomposition of streamflow timeseries. The horizontal axis represents the period length of oscillations in streamflow timeseries on a logarithmic scale, while the vertical axis represents the spectral power, a unit that can be intuitively understood as how much a given timescale contributes to the variance in the data.

3.3 Identifying controls on streamflow regime with PCA metrics

Three types of machine learning models corroboratively suggested that just a few catchment characteristics control flow regime (as measured by the PCA metrics, supplemental figure S8). These included dominant contributions of cumulative precipitation for PCA metrics 1, 5, and 7, catchment area for metric 2, climate variables for metrics 3 and 4, and land cover for metrics 3, 5, and 6. In addition, the length of the timeseries was an important feature for several metrics. The r-squared values across models decreased from the higher variance-explaining metrics to the lower variance explaining metrics. Specifically, model accuracy decreased from a maximum of ~0.85 for metric 1 to a maximum of ~0.45 for metric 7 (supplemental figure S8). To visualize the relationship between flow metrics and the subset of catchment characteristics that the machine learning analysis suggested were important, as well as catchment characteristics

suggested to be important by hydrological theory, we plotted the relationships between the PCA metrics and selected catchment characteristics (figures 7 and 8). The dominant role of catchment size was quite clear, including non-linear relationships between catchment size and metrics 3, 5, and 7, in which the largest streams tended to behave similarly to the smallest streams. Relationships between biomes were surprisingly ambiguous given that biome delineations are defined by temperature and precipitation. However, when split, temperature and precipitation showed relationships to the flow metrics, whereas the effect imposed by land use such as forest cover and net human alterations was less visible (figure 8). A more comprehensive set of visualizations across a broader range of catchment characteristics can be found in supplemental figures S10-S13.

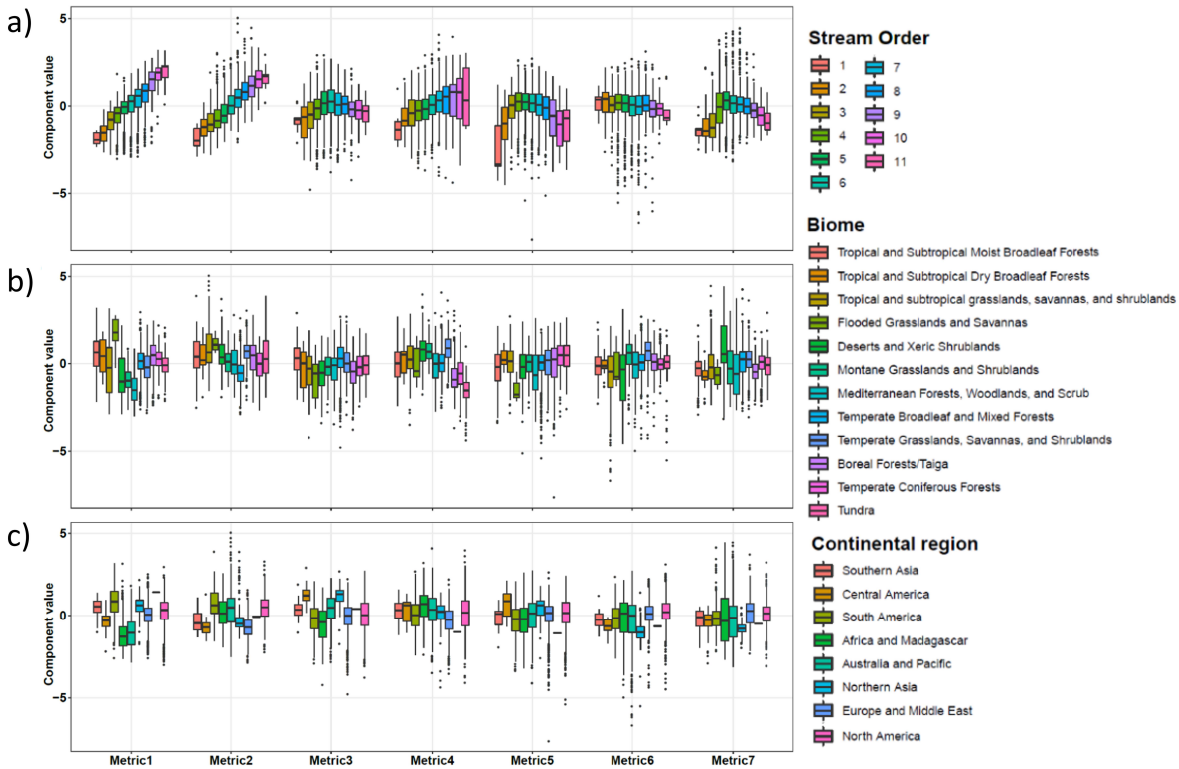

Figure 7. The 7 PCA flow metrics divided according to a) stream order, b) biome, and c) continental region. Box plots are constructed using standard conventions: boxes are the range of the 1st through 3rd quartiles, lines represent the range between the minimum and maximum values when these values are within 1.5 times the inter-quartile range (IQR), and dots represent outliers beyond 1.5 IQR. Note that the relationship between stream order and flow regime is much stronger than the relationship between biome and flow regime across most metrics, and that continental region was an even poorer predictor of flow regime. Also note the non-linear relationship between stream order and several of the PCA metrics.

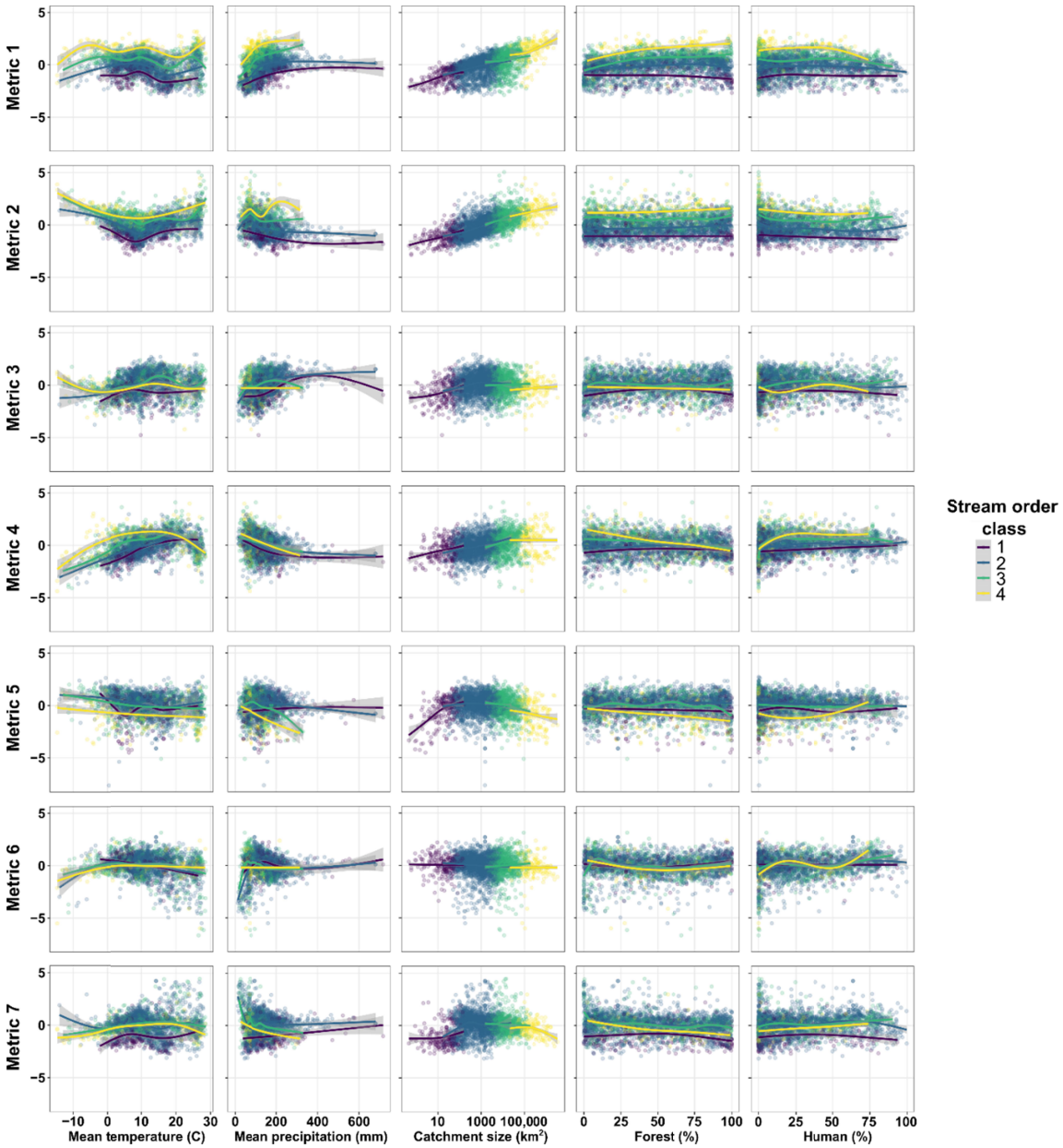

Figure 8. Continuous relationships between 7 PCA flow metrics and catchment properties of mean annual temperature, mean annual precipitation (normalized for catchment size), catchment size, percent forest cover, and percent human influence. Streams have been colored according to stream order (with group 4 representing the largest catchments). The plots demonstrate the coherence of the relationship between catchment size and streamflow regime, while highlighting the comparatively weak relationship between human and forest cover and flow regime. Also of note are the complex, non-linear relationships between temperature and precipitation and the 7 flow metrics.

3.4 Identifying controls on streamflow regime with Frequency Decompositions

Many of the drivers of flow regime suggested by the PCA flow metrics were also highlighted by the wavelet analysis (figure 9). For example, catchment size was natively correlated with high frequency (short-term) phenomena but positively correlated with low frequency (long-term) phenomena. Temperature followed a more complex relationship where

high winter temperatures were positively correlated with multi-day phenomena and negatively correlated with multi-month to year-long phenomena. In contrast, summer temperatures most strongly correlated with multi-year phenomena. Many land-use characteristics followed similar complex relationships across multiple timescales (supplemental figure S14).

Machine learning models trained to predict spectral power using catchment characteristics consistently suggested that climate was the most important predictor, followed by land cover and catchment area, with human impact becoming increasingly important at longer timescales (figure 10). Against expectations, dams were not particularly important predictors of flow regime (supplemental figures S14 and S15). In addition, variability at shorter timescales was easier to predict that variability at longer timescales (supplemental figure S16).

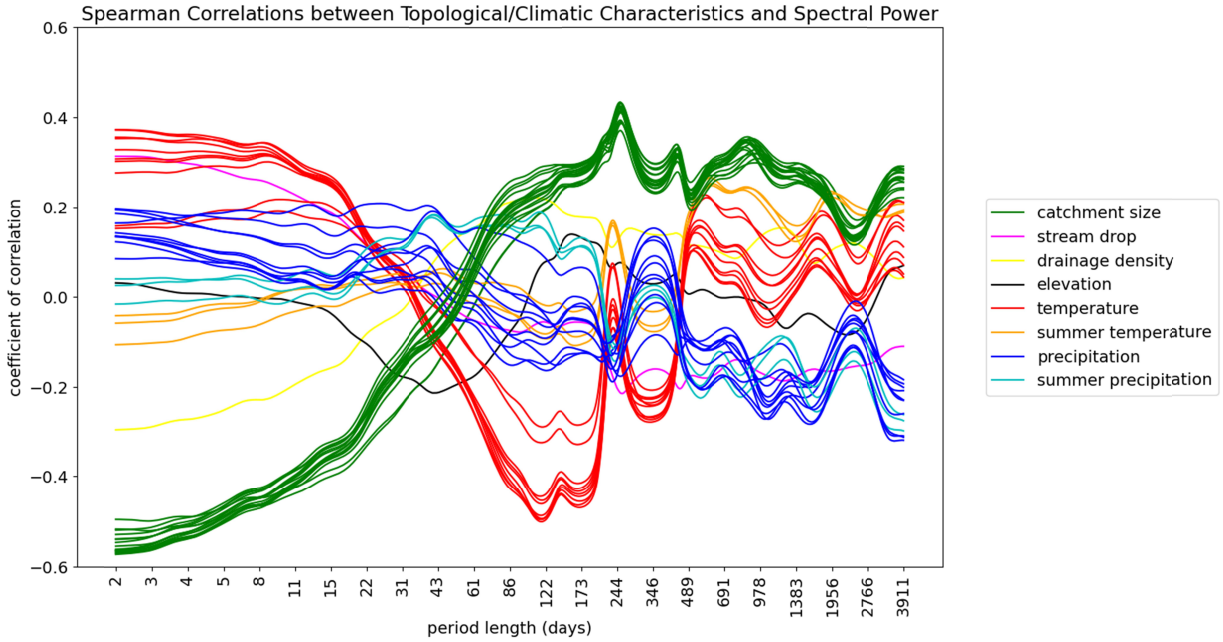

Figure 9. Correlations between catchment characteristics and spectral power across period lengths ranging from two days to almost ten years.

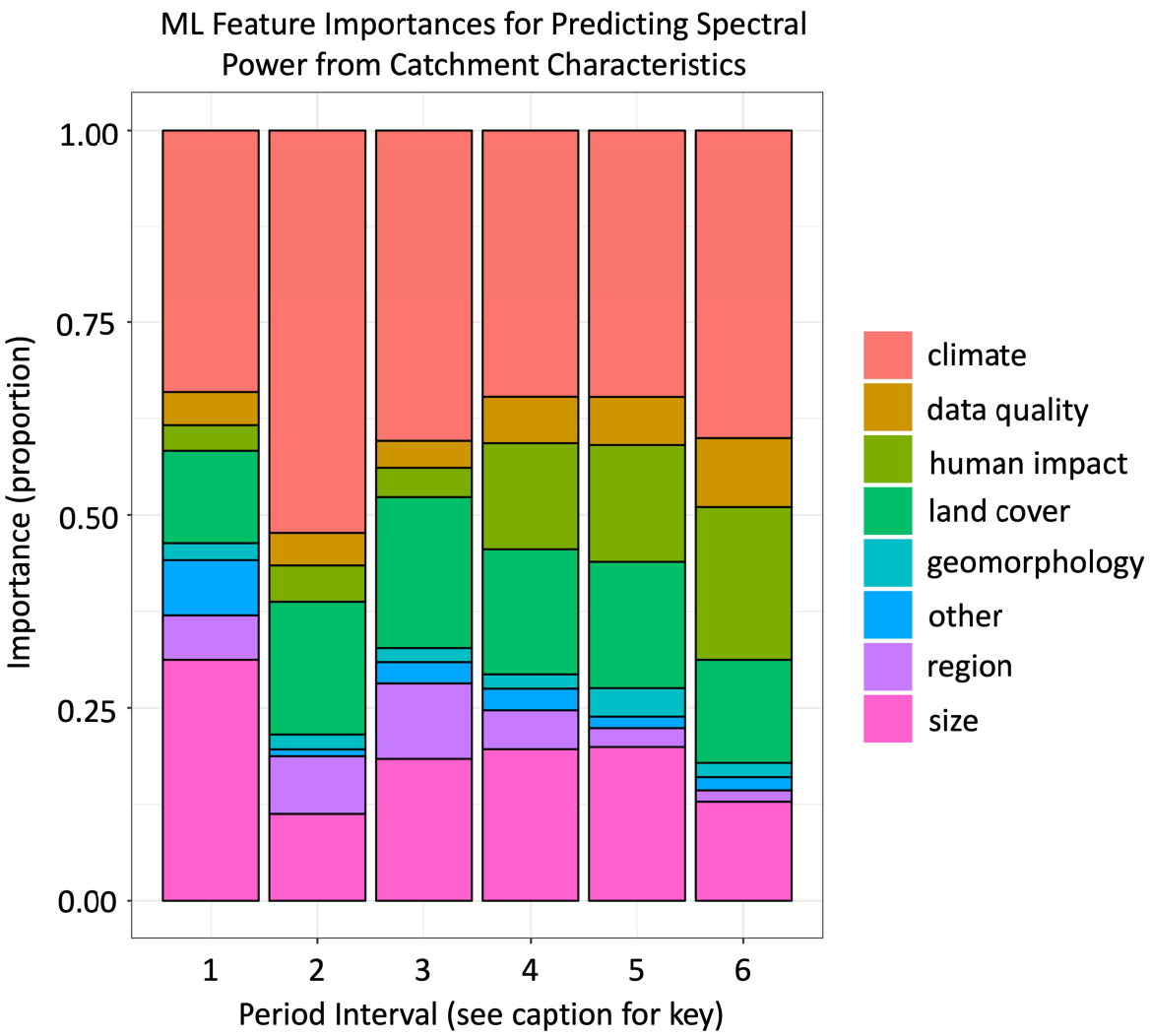

Figure 10. Feature importances of machine learning models trained to predict mean spectral power across different intervals (1: 2-40 days, 2: 41-180 days, 3: 181-365 days, 4: 366-1,095 days, 5: 1,096-2,190 days, and 6: 2,191-10,000 days) using catchment characteristics data. For simplicity, catchment characteristics have been grouped into 8 categories. The relative contribution of each category to the predictive power of the models is represented by the height of each bar.

4 Discussion

River networks connect and unite much of life on Earth, including human societies (Figure 1). Like a constellation of linked ecological heartbeats, river flows rise and fall across myriad timescales, sculpting aquatic habitat, driving biogeochemical flux, and quenching human water needs. In an increasingly human-dominated world of dams, agricultural water use, and changing climate, it is critical to understand patterns in hydrological processes at planetary scales, and to identify which climate, land cover, and water-use factors in turn drive those patterns. One of the necessary milestones needed to achieve this understanding has been the development of a quantitative language for describing streamflow regime that is both concise enough to favor meaningful insight, yet broad enough to capture the wide range of behaviors

seen in streams around the world. Therefore, our primary purpose in this paper was to explore possible methods for describing streamflow regime, and then to leverage those methods to identify patterns in and drivers of flow regime. Given the complexity that is traditionally attributed to streamflow regime (Dey & Mujumdar, 2022; Sivapalan, 2006; Tetzlaff et al., 2008), the large number of different hydrological models (Horton et al., 2022), and the number of parameters these models usually take (Dhami & Pandey, 2019), we were surprised by the low-dimensionality (i.e. simplicity) that global streamflow data consistently expressed through a variety of analyses. At its core, this low dimensionality was driven by linkages of streamflow properties between timescales. Below, we discuss our findings in light of current ecological challenges and hydrological theory, with particular emphasis on the importance of understanding timescales as interacting units with low effective dimensionality.

4.1 Are streamflow metrics or frequency decompositions better?

Streamflow metrics and frequency decompositions such as wavelet analyses facilitate different, albeit related insights into streamflow regime. Streamflow metrics are not limited by a strict mathematical framework and therefore describe a wide range of phenomena, including variability, timing, and volume of flow with precise, albeit poorly organized, detail. Data-driven techniques such as PCA can counter this disorganization by identifying latent low-dimensional structure in streamflow metrics. One of the key contributions of this work was to apply data-driven structure identification techniques to unmodeled streamflow data at a global scale. Indeed, PCA analysis suggested that globally, streamflow metrics are inherently compressible along linear manifolds, with 68% of the variability in flow data explained by 7 linear principal components. However, our analysis also showed that a substantial portion of the information provided by streamflow metrics (the remaining 32%) is not well described by linear structures. In other words, streamflow metrics, and by extensions streamflow data, contain an inherently information rich component, and thus the large number of metrics used to describe streamflow is well-justified. We suggest that streamflow is both a simple and complex phenomenon, with minor, complex (high-dimensional) structures emerging on top of the dominant, simple (low-dimensional) patterns that are consistent at global scales. This dominant compressibility has previously been attributed to redundancy in streamflow metrics (Olden and Poff 2003)—not an unlikely outcome given the sheer number of metrics available. However, the disorganization inherent within this approach also belies that the dominant low-dimensional structure is in-part a manifestation of linkages in flow properties among timescales. Identifying these linkages is another key contribution of this work. Our results suggest that these linkages arise from a small number of hydrological phenomena that are tuned by relatively few catchment properties such as drainage basin size, mean annual temperature, precipitation, and land use. Streamflow metrics fail to identify these linkages because they have not traditionally been organized by timescale and analyzed as an interacting set of variables. This is one of the great advantages of frequency decompositions—they organize phenomena in a timeseries by their duration, from days to decades. Complex dynamics are quantified with a concise vocabulary: the amplitude, phase, waveform, and vertical shift of waves of varying frequency. This vocabulary resides at a level of abstraction that is perhaps uncomfortably distant from real-world biogeochemical cycling but that is nonetheless remarkably useful for organizing structure in data, identifying processes and interactions that would otherwise be invisible.

We further suggest that as biogeochemical datasets increase in temporal and spatial scales, data-driven descriptors based on low-dimensional structure are key for several reasons: 1) they provide sanity checks of intuitive notions or concepts common in sub-disciplines that are otherwise quantitatively unfalsifiable (Kipper, 2021). For example, in hydrology the notions of "semi-arid watersheds" and "snow-driven watersheds" are commonly employed in the literature (Arheimer et al., 2017; Cosh et al., 2008; Manning et al., 2022; Poon & Kinoshita, 2018). We suggest that these intuitive concepts represent informal, expert-driven versions of dimension reduction (Bates, 2020; Wolff, 2019). Confirming that our expert-derived vernacular corresponds to patterns in data is critical as policy decisions are made regarding restoration efforts and global climate-change action. 2) Correlating low-dimensional structure with system characteristics is a first step towards developing understandable, causal mathematical models that can more reliably be used to predict system behavior under novel conditions such as climate change. We distinguish data-driven descriptors (low-dimensional structure) from data-driven models, which tend to be black-box models whose generalizability to novel conditions is harder to verify (Rudin, 2019). 3) Low-dimensional structure forms a concise vocabulary for communicating major issues to non-experts (see (Eckmann & Tlusty, 2021; Lum et al., 2013; Nicolau et al., 2011) for examples from other fields), significantly aiding interdisciplinary discussions. In the realm of biogeochemistry, where so many organisms, processes, and societal communities are involved, succinct communication is key for progress to be made in the face of increasing environmental degradation (Abbott, Bishop, Zarnetske, Hannah, et al., 2019; Frei et al., 2021).

4.2 Streamflow Metrics Can be Predicted from Temperature, Precipitation, and Catchment Size

Multiple analyses independently suggested that only a few catchment properties (temperature, precipitation, and catchment size) were necessary for predicting the dominant structures in streamflow regime data. This was true regardless of the method used for quantifying flow regime. For example, three types of machine learning models suggested that PCA flow metrics could be predicted almost exclusively from temperature, precipitation, and catchment area. When plotted together, the relationships between PCA flow metrics and these variables were visually obvious, while the relationships between PCA flow metrics and variables not identified as important by the machine learning models (e.g., forest cover, biome) were markedly less clear. Similar patterns emerged when a wavelet analysis was used to quantify flow regime: machine learning analyses consistently identified climate and catchment size as important predictors of flow variability at all temporal scales considered. Visualizations of the correlations between these predictors and the frequency domain corroborated these results. However, there was one important difference between features that were important for predicting PCA flow metrics and frequency decompositions – the influence of land use. This category grouped several variables, including percent forest cover, percent shrub, percent snow, etc. into a single label. And while individual land use characteristics were not particularly important in isolation, machine learning models consistently ranked this group as a whole to be as important as catchment area for predicting variability in flow at all timescales longer than a few months. We speculate that precipitation, temperature, and catchment size may regulate near-universal hydrological processes that are responsible for the highly compressible components of streamflow regime (those captured by the 7 PCA metrics) (Giano, 2021; N. LeRoy Poff et al., 1997), and that the more complicated ecohydrological interactions introduced by the myriad possible land use regimes and geological factors are responsible for streamflow properties that

were harder to identify with PCA analysis (Bladon et al., 2014; Manning et al., 2022; Tague & Grant, 2004; Wu et al., 2021)—though we note that land use is likely correlated with climatic and geological factors. Said differently, our results imply that a simple, emergent physics may exist at the catchment scale, where a handful of mean catchment properties accurately predict flashiness, timing, and volume of flow at the basin's outlet, to the extent that biological interactions remain simple (Sposito, 2017; Zhou et al., 2015).

Interestingly, dams were not an important predictor of flow regime for any analysis, which runs contrary to previous results (Arheimer et al., 2017). They did correlate with several flow metrics, PCA metrics, and certain timescales as indicated by wavelet analysis. However, in no case were they a primary predictor of flow regime according to multiple machine learning analyses. This may be because dam number and dam surface area correlate more strongly with catchment area than any other catchment characteristic; there are very few large rivers that are not heavily dammed (with significant impacts on global biogeochemical cycling, (Maavara et al., 2020). It may also be that the signal dampening that occurs in large catchments is more influential than the dynamics introduced by human dam management (Chezik et al., 2017), or conversely, that dams contribute little to very high flow events wherein dams spill over and large amounts of water go downstream regardless. Separating cause from correlation in this context may be impossible. Concordantly, one of the major goals of this work was to use observed streamflow data to characterize the drivers of streamflow regime in the context of human domination of the water cycle (Abbott, Bishop, Zarnetske, Hannah, et al., 2019; Chalise et al., 2021; Palmer & Ruhi, 2019). And while it is ambiguous from these results whether a drainage basin's area has a larger impact than that imposed by dams, our results strongly suggest that human alterations to earth's climate and land surface have the potential to impact river flow to a degree that is equal to if not greater than that imposed by the construction of dams (Nijssen et al., 2001; Schneider et al., 2013; Wenger et al., 2011; Xenopoulos & Lodge, 2006).

5 Conclusions

In closing, river flow is a critical component of biogeochemical cycling and ecosystem functioning (Palmer & Ruhi, 2019). Given the massive scale of human alterations to the water cycle, it has never been more important to understand how climatic, geomorphological, biological, and industrial factors interact to mediate the rise and fall of rivers. We propose that river flow can only be understood as a phenomenon occurring across many *interacting* timescales. These interactions are visible through stunning low-dimensional structure in streamflow data that correlates closely with a small number of catchment characteristics. Together, these results suggest that global river flow dynamics are controlled by just a few dominant hydrological mechanisms that are locally tuned by land use, geology, and human infrastructure. The implications of organizing low-dimensional structure within streamflow data for biogeochemical cycling are broad and far reaching, inasmuch as simplicity provides a *lingua franca* for the diverse academic and societal communities whose livelihoods pulse to the rhythm of earth's rivers and streams.

Acknowledgments

This project was funded by the U.S. National Science Foundation (grant numbers DEB-1354867, EAR-2011439, EAR-2012123) and the Utah Division of Natural Resources Watershed Restoration Initiative. We thank the Stream Resiliency Research Coordination Network for initiating and coordinating this collaboration.

Data Availability

The data used in this study are available on researchgate.net at https://doi.org/10.13140/RG.2.2.24985.95842 and https://doi.org/10.13140/RG.2.2.31696.84487 under CC BY 4.0 licenses.

References

Abbott, B. W., Gruau, G., Zarnetske, J. P., Moatar, F., Barbe, L., Thomas, Z., et al. (2018). Unexpected spatial stability of water chemistry in headwater stream networks. *Ecology Letters*, *21*(2), 296–308. https://doi.org/10.1111/ele.12897

Abbott, B. W., Bishop, K., Zarnetske, J. P., Hannah, D. M., Frei, R. J., Minaudo, C., et al. (2019). A water cycle for the Anthropocene. *Hydrological Processes*, *33*(23), 3046–3052. https://doi.org/10.1002/hyp.13544

Abbott, B. W., Bishop, K., Zarnetske, J. P., Minaudo, C., Chapin, F. S., Krause, S., et al. (2019). Human domination of the global water cycle absent from depictions and perceptions. *Nature Geoscience*, *12*(7), 533–540. https://doi.org/10.1038/s41561-019-0374-y

Alfieri, L., Lorini, V., Hirpa, F. A., Harrigan, S., Zsoter, E., Prudhomme, C., & Salamon, P. (2020). A global streamflow reanalysis for 1980–2018. *Journal of Hydrology X*, *6*, 100049. https://doi.org/10.1016/j.hydroa.2019.100049

Archfield, S. A., Kennen, J. G., Carlisle, D. M., & Wolock, D. M. (2014). An objective and parsimonious approach for classifying natural flow regimes at a continental scale. *River Research and Applications*, *30*(9), 1166–1183. https://doi.org/10.1002/rra.2710

Arheimer, B., Donnelly, C., & Lindström, G. (2017). Regulation of snow-fed rivers affects flow regimes more than climate change. *Nature Communications*, *8*(1), 62. https://doi.org/10.1038/s41467-017-00092-8

Ascott, M. J., Gooddy, D. C., Fenton, O., Vero, S., Ward, R. S., Basu, N. B., et al. (2021). The need to integrate legacy nitrogen storage dynamics and time lags into policy and practice.

Science of The Total Environment, *781*, 146698. https://doi.org/10.1016/j.scitotenv.2021.146698

Barbarossa, V., Huijbregts, M. A. J., Beusen, A. H. W., Beck, H. E., King, H., & Schipper, A. M. (2018). FLO1K, global maps of mean, maximum and minimum annual streamflow at 1 km resolution from 1960 through 2015. *Scientific Data*, *5*(1), 180052. https://doi.org/10.1038/sdata.2018.52

Bates, C. (2020). Efficient data compression in human perception. Retrieved from https://urresearch.rochester.edu/institutionalPublicationPublicView.action?institutionalItemId=35450

Berghuijs, W. R., Harrigan, S., Molnar, P., Slater, L. J., & Kirchner, J. W. (2019). The Relative Importance of Different Flood-Generating Mechanisms Across Europe. *Water Resources Research*, *0*(0). https://doi.org/10.1029/2019WR024841

Bernhardt, E. S., Rosi, E. J., & Gessner, M. O. (2017). Synthetic chemicals as agents of global change. *Frontiers in Ecology and the Environment*, *15*(2), 84–90. https://doi.org/10.1002/fee.1450

Biau, G., & Scornet, E. (2016). A random forest guided tour. *TEST*, *25*(2), 197–227. https://doi.org/10.1007/s11749-016-0481-7

Bladon, K. D., Emelko, M. B., Silins, U., & Stone, M. (2014). Wildfire and the Future of Water Supply. *Environmental Science & Technology*, *48*(16), 8936–8943. https://doi.org/10.1021/es500130g

Bochet, O., Bethencourt, L., Dufresne, A., Farasin, J., Pédrot, M., Labasque, T., et al. (2020). Iron-oxidizer hotspots formed by intermittent oxic–anoxic fluid mixing in fractured rocks. *Nature Geoscience*, 1–7. https://doi.org/10.1038/s41561-019-0509-1

715 Breiman, L. (2001). Random Forests. *Machine Learning*, *45*(1), 5–32.
716 https://doi.org/10.1023/A:1010933404324
717 Bunn, S. E., & Arthington, A. H. (2002). Basic Principles and Ecological Consequences of
718 Altered Flow Regimes for Aquatic Biodiversity. *Environmental Management*, *30*(4),
719 492–507. https://doi.org/10.1007/s00267-002-2737-0
720 Carey, S. K., Tetzlaff, D., Buttle, J., Laudon, H., McDonnell, J., McGuire, K., et al. (2013). Use
721 of color maps and wavelet coherence to discern seasonal and interannual climate
722 influences on streamflow variability in northern catchments. *Water Resources Research*,
723 *49*(10), 6194–6207. https://doi.org/10.1002/wrcr.20469
724 Carlisle, D. M., Falcone, J., Wolock, D. M., Meador, M. R., & Norris, R. H. (2010). Predicting
725 the natural flow regime: models for assessing hydrological alteration in streams. *River*
726 *Research and Applications*, *26*(2), 118–136. https://doi.org/10.1002/rra.1247
727 Chalise, D. R., Sankarasubramanian, A., & Ruhi, A. (2021). Dams and Climate Interact to Alter
728 River Flow Regimes Across the United States. *Earth's Future*, *9*(4), e2020EF001816.
729 https://doi.org/10.1029/2020EF001816
730 Chezik, K. A., Anderson, S. C., & Moore, J. W. (2017). River networks dampen long-term
731 hydrological signals of climate change. *Geophysical Research Letters*, *44*(14), 7256–
732 7264. https://doi.org/10.1002/2017GL074376
733 Cosh, M. H., Jackson, T. J., Moran, S., & Bindlish, R. (2008). Temporal persistence and stability
734 of surface soil moisture in a semi-arid watershed. *Remote Sensing of Environment*,
735 *112*(2), 304–313. https://doi.org/10.1016/j.rse.2007.07.001
736 Dey, P., & Mujumdar, P. (2022). On the statistical complexity of streamflow. *Hydrological*
737 *Sciences Journal*, *67*(1), 40–53. https://doi.org/10.1080/02626667.2021.2000991

738 Dhami, B., & Pandey, A. (2019). Comparative Review of Recently Developed Hydrological
739 Models.
740 Díaz, S., Settele, J., Brondízio, E. S., Ngo, H. T., Agard, J., Arneth, A., et al. (2019). Pervasive
741 human-driven decline of life on Earth points to the need for transformative change.
742 *Science*, *366*(6471). https://doi.org/10.1126/science.aax3100
743 Döll, P., & Schmied, H. M. (2012). How is the impact of climate change on river flow regimes
744 related to the impact on mean annual runoff? A global-scale analysis. *Environmental*
745 *Research Letters*, *7*(1), 014037. https://doi.org/10.1088/1748-9326/7/1/014037
746 Dupas, R., Abbott, B. W., Minaudo, C., & Fovet, O. (2019). Distribution of Landscape Units
747 Within Catchments Influences Nutrient Export Dynamics. *Frontiers in Environmental*
748 *Science*, *7*. Retrieved from https://www.frontiersin.org/article/10.3389/fenvs.2019.00043
749 Eckmann, J.-P., & Tlusty, T. (2021). Dimensional reduction in complex living systems: Where,
750 why, and how. *BioEssays*, *43*(9), 2100062. https://doi.org/10.1002/bies.202100062
751 Elith, J., Leathwick, J. R., & Hastie, T. (2008). A working guide to boosted regression trees.
752 *Journal of Animal Ecology*, *77*(4), 802–813. https://doi.org/10.1111/j.1365-
753 2656.2008.01390.x
754 Fisher, S. G., Grimm, N. B., Martí, E., Holmes, R. M., & Jones Jr, J. B. (1998). Material
755 spiraling in stream corridors: a telescoping ecosystem model. *Ecosystems*, *1*(1), 19–34.
756 Frei, R. J., Abbott, B. W., Dupas, R., Gu, S., Gruau, G., Thomas, Z., et al. (2020). Predicting
757 Nutrient Incontinence in the Anthropocene at Watershed Scales. *Frontiers in*
758 *Environmental Science*, *7*. https://doi.org/10.3389/fenvs.2019.00200

759 Frei, R. J., Lawson, G. M., Norris, A. J., Cano, G., Vargas, M. C., Kujanpää, E., et al. (2021).
760 Limited progress in nutrient pollution in the U.S. caused by spatially persistent nutrient
761 sources. *PLOS ONE*, *16*(11), e0258952. https://doi.org/10.1371/journal.pone.0258952
762 George, R., McManamay, R., Perry, D., Sabo, J., & Ruddell, B. L. (2021). Indicators of hydro-
763 ecological alteration for the rivers of the United States. *Ecological Indicators*, *120*,
764 106908. https://doi.org/10.1016/j.ecolind.2020.106908
765 Gerten, D., Rost, S., von Bloh, W., & Lucht, W. (2008). Causes of change in 20th century global
766 river discharge. *Geophysical Research Letters*, *35*(20), L20405.
767 https://doi.org/10.1029/2008GL035258
768 Giano, S. I. (2021). Fluvial Geomorphology and River Management. *Water*, *13*(11), 1608.
769 https://doi.org/10.3390/w13111608
770 Gleeson, T., Wang-Erlandsson, L., Porkka, M., Zipper, S. C., Jaramillo, F., Gerten, D., et al.
771 (2020). Illuminating water cycle modifications and Earth system resilience in the
772 Anthropocene. *Water Resources Research*, *56*(4), e2019WR024957.
773 https://doi.org/10.1029/2019WR024957
774 Gnann, S. J., Coxon, G., Woods, R. A., Howden, N. J. K., & McMillan, H. K. (2021). TOSSH: A
775 Toolbox for Streamflow Signatures in Hydrology. *Environmental Modelling and*
776 *Software*, *138*, 104983. https://doi.org/10.1016/j.envsoft.2021.104983
777 Godsey, S. E., & Kirchner, J. W. (2014). Dynamic, discontinuous stream networks:
778 hydrologically driven variations in active drainage density, flowing channels and stream
779 order. *Hydrological Processes*, *28*(23), 5791–5803. https://doi.org/10.1002/hyp.10310

780 Gorski, G., & Zimmer, M. A. (2021). Hydrologic regimes drive nitrate export behavior in
781 human-impacted watersheds. *Hydrology and Earth System Sciences*, *25*(3), 1333–1345.
782 https://doi.org/10.5194/hess-25-1333-2021
783 Hain, E. F., Kennen, J. G., Caldwell, P. V., Nelson, S. A. C., Sun, G., & McNulty, S. G. (2018).
784 Using regional scale flow–ecology modeling to identify catchments where fish
785 assemblages are most vulnerable to changes in water availability. *Freshwater Biology*,
786 *63*(8), 928–945. https://doi.org/10.1111/fwb.13048
787 Hales, R. C., Nelson, E. J., Souffront, M., Gutierrez, A. L., Prudhomme, C., Kopp, S., et al.
788 (n.d.). Advancing global hydrologic modeling with the GEOGloWS ECMWF streamflow
789 service. *Journal of Flood Risk Management*, *n/a*(n/a), e12859.
790 https://doi.org/10.1111/jfr3.12859
791 Hannah, D. M., Demuth, S., Lanen, H. A. J. van, Looser, U., Prudhomme, C., Rees, G., et al.
792 (2011). Large-scale river flow archives: importance, current status and future needs.
793 *Hydrological Processes*, *25*(7), 1191–1200. https://doi.org/10.1002/hyp.7794
794 Harrison, I., Abell, R., Darwall, W., Thieme, M. L., Tickner, D., & Timboe, I. (2018). The
795 freshwater biodiversity crisis. *Science*, *362*(6421), 1369–1369.
796 https://doi.org/10.1126/science.aav9242
797 Helton, A. M., Poole, G. C., Meyer, J. L., Wollheim, W. M., Peterson, B. J., Mulholland, P. J., et
798 al. (2011). Thinking outside the channel: modeling nitrogen cycling in networked river
799 ecosystems. *Frontiers in Ecology and the Environment*, *9*(4), 229–238.
800 https://doi.org/10.1890/080211

Hogeboom, R. J., de Bruin, D., Schyns, J. F., Krol, M. S., & Hoekstra, A. Y. (2020). Capping Human Water Footprints in the World's River Basins. *Earth's Future*, *8*(2), e2019EF001363. https://doi.org/10.1029/2019EF001363

Horton, P., Schaefli, B., & Kauzlaric, M. (2022). Why do we have so many different hydrological models? A review based on the case of Switzerland. *WIREs Water*, *9*(1), e1574. https://doi.org/10.1002/wat2.1574

Jones, N. E., Schmidt, B. J., & Melles, S. J. (2014). Characteristics and distribution of natural flow regimes in Canada: a habitat template approach. *Canadian Journal of Fisheries and Aquatic Sciences*, *71*(11), 1616–1624. https://doi.org/10.1139/cjfas-2014-0040

Kipper, J. (2021). Intuition, intelligence, data compression. *Synthese*, *198*(27), 6469–6489. https://doi.org/10.1007/s11229-019-02118-8

Labat, D. (2010). Cross wavelet analyses of annual continental freshwater discharge and selected climate indices. *Journal of Hydrology*, *385*(1), 269–278. https://doi.org/10.1016/j.jhydrol.2010.02.029

Lane, B. A., Dahlke, H. E., Pasternack, G. B., & Sandoval-Solis, S. (2017). Revealing the Diversity of Natural Hydrologic Regimes in California with Relevance for Environmental Flows Applications. *JAWRA Journal of the American Water Resources Association*, *53*(2), 411–430. https://doi.org/10.1111/1752-1688.12504

Levia, D. F., Creed, I. F., Hannah, D. M., Nanko, K., Boyer, E. W., Carlyle-Moses, D. E., et al. (2020). Homogenization of the terrestrial water cycle. *Nature Geoscience*, *13*(10), 656–658. https://doi.org/10.1038/s41561-020-0641-y

822 Lin, P., Pan, M., Beck, H. E., Yang, Y., Yamazaki, D., Frasson, R., et al. (2019). Global
823 Reconstruction of Naturalized River Flows at 2.94 Million Reaches. *Water Resources*
824 *Research*, *55*(8), 6499–6516. https://doi.org/10.1029/2019WR025287
825 Liu, J., Zhang, Q., Singh, V. P., Song, C., Zhang, Y., Sun, P., & Gu, X. (2018). Hydrological
826 effects of climate variability and vegetation dynamics on annual fluvial water balance in
827 global large river basins. *Hydrology and Earth System Sciences*, *22*(7), 4047–4060.
828 https://doi.org/10.5194/hess-22-4047-2018
829 Liu, S., Kuhn, C., Amatulli, G., Aho, K., Butman, D. E., Allen, G. H., et al. (2022). The
830 importance of hydrology in routing terrestrial carbon to the atmosphere via global
831 streams and rivers. *Proceedings of the National Academy of Sciences*, *119*(11),
832 e2106322119. https://doi.org/10.1073/pnas.2106322119
833 Lum, P. Y., Singh, G., Lehman, A., Ishkanov, T., Vejdemo-Johansson, M., Alagappan, M., et al.
834 (2013). Extracting insights from the shape of complex data using topology. *Scientific*
835 *Reports*, *3*(1), 1236. https://doi.org/10.1038/srep01236
836 Maavara, T., Chen, Q., Van Meter, K., Brown, L. E., Zhang, J., Ni, J., & Zarfl, C. (2020). River
837 dam impacts on biogeochemical cycling. *Nature Reviews Earth & Environment*, *1*(2),
838 103–116. https://doi.org/10.1038/s43017-019-0019-0
839 Malone, E. T., Abbott, B. W., Klaar, M. J., Kidd, C., Sebilo, M., Milner, A. M., & Pinay, G.
840 (2018). Decline in Ecosystem δ13C and Mid-Successional Nitrogen Loss in a Two-
841 Century Postglacial Chronosequence. *Ecosystems*, *21*(8), 1659–1675.
842 https://doi.org/10.1007/s10021-018-0245-1

843 Manning, A. L., Harpold, A., & Csank, A. (2022). Spruce Beetle Outbreak Increases Streamflow
844 From Snow-Dominated Basins in Southwest Colorado, USA. *Water Resources Research*,
845 *58*(5), e2021WR029964. https://doi.org/10.1029/2021WR029964
846 Masaki, Y., Hanasaki, N., Biemans, H., Schmied, H. M., Tang, Q., Yoshihide Wada, et al.
847 (2017). Intercomparison of global river discharge simulations focusing on dam
848 operation—multiple models analysis in two case-study river basins, Missouri–Mississippi
849 and Green–Colorado. *Environmental Research Letters*, *12*(5), 055002.
850 https://doi.org/10.1088/1748-9326/aa57a8
851 McMahon, T. A., Vogel, R. M., Peel, M. C., & Pegram, G. G. S. (2007). Global streamflows –
852 Part 1: Characteristics of annual streamflows. *Journal of Hydrology*, *347*(3), 243–259.
853 https://doi.org/10.1016/j.jhydrol.2007.09.002
854 McMillan, H. (2021). A review of hydrologic signatures and their applications. *WIREs Water*.
855 https://doi.org/10.1002/wat2.1499
856 Minaudo, C., Dupas, R., Gascuel-Odoux, C., Fovet, O., Mellander, P.-E., Jordan, P., et al.
857 (2017). Nonlinear empirical modeling to estimate phosphorus exports using continuous
858 records of turbidity and discharge: P EXPORTS FROM TURBIDITY AND
859 DISCHARGE. *Water Resources Research*, *53*(9), 7590–7606.
860 https://doi.org/10.1002/2017WR020590
861 Moatar, F., Abbott, B. W., Minaudo, C., Curie, F., & Pinay, G. (2017). Elemental properties,
862 hydrology, and biology interact to shape concentration-discharge curves for carbon,
863 nutrients, sediment, and major ions. *Water Resources Research*, *53*(2), 1270–1287.
864 https://doi.org/10.1002/2016WR019635

865 Myles, A. J., Feudale, R. N., Liu, Y., Woody, N. A., & Brown, S. D. (2004). An introduction to
866 decision tree modeling. *Journal of Chemometrics*, *18*(6), 275–285.
867 https://doi.org/10.1002/cem.873
868 Nicolau, M., Levine, A. J., & Carlsson, G. (2011). Topology based data analysis identifies a
869 subgroup of breast cancers with a unique mutational profile and excellent survival.
870 *Proceedings of the National Academy of Sciences*, *108*(17), 7265–7270.
871 https://doi.org/10.1073/pnas.1102826108
872 Nijssen, B., O'Donnell, G. M., Hamlet, A. F., & Lettenmaier, D. P. (2001). Hydrologic
873 Sensitivity of Global Rivers to Climate Change. *Climatic Change*, *50*(1), 143–175.
874 https://doi.org/10.1023/A:1010616428763
875 Olden, J. D., & Poff, N. L. (2003). Redundancy and the choice of hydrologic indices for
876 characterizing streamflow regimes. *River Research and Applications*, *19*(2), 101–121.
877 https://doi.org/10.1002/rra.700
878 Oldfield, J. D. (2016). Mikhail Budyko's (1920–2001) contributions to Global Climate Science:
879 from heat balances to climate change and global ecology. *Wiley Interdisciplinary*
880 *Reviews: Climate Change*, *7*(5), 682–692. https://doi.org/10.1002/wcc.412
881 Palmer, M., & Ruhi, A. (2019). Linkages between flow regime, biota, and ecosystem processes:
882 Implications for river restoration. *Science*, *365*(6459).
883 https://doi.org/10.1126/science.aaw2087
884 Pedregosa, F., Varoquaux, G., Gramfort, A., Michel, V., Thirion, B., Grisel, O., et al. (2011).
885 Scikit-learn: Machine Learning in Python. *Journal of Machine Learning Research*, *12*, 6.
886 Pinay, G., Bernal, S., Abbott, B. W., Lupon, A., Marti, E., Sabater, F., & Krause, S. (2018).
887 Riparian Corridors: A New Conceptual Framework for Assessing Nitrogen Buffering

Across Biomes. *Frontiers in Environmental Science*, *6*. https://doi.org/10.3389/fenvs.2018.00047

Poff, N. Leroy, & Zimmerman, J. K. H. (2010). Ecological responses to altered flow regimes: a literature review to inform the science and management of environmental flows. *Freshwater Biology*, *55*(1), 194–205. https://doi.org/10.1111/j.1365-2427.2009.02272.x

Poff, N. LeRoy, Allan, J. D., Bain, M. B., Karr, J. R., Prestegaard, K. L., Richter, B. D., et al. (1997). The Natural Flow Regime. *BioScience*, *47*(11), 769–784. https://doi.org/10.2307/1313099

Poon, P. K., & Kinoshita, A. M. (2018). Spatial and temporal evapotranspiration trends after wildfire in semi-arid landscapes. *Journal of Hydrology*, *559*, 71–83. https://doi.org/10.1016/j.jhydrol.2018.02.023

Raymond, P. A., Saiers, J. E., & Sobczak, W. V. (2016). Hydrological and biogeochemical controls on watershed dissolved organic matter transport: pulse-shunt concept. *Ecology*, *97*(1), 5–16. https://doi.org/10.1890/14-1684.1

Reaver, N. G. F., Kaplan, D. A., Klammler, H., & Jawitz, J. W. (2020). Reinterpreting the Budyko Framework. *Hydrology and Earth System Sciences Discussions*, 1–31. https://doi.org/10.5194/hess-2020-584

Rudin, C. (2019). Stop explaining black box machine learning models for high stakes decisions and use interpretable models instead. *Nature Machine Intelligence*, *1*(5), 206–215. https://doi.org/10.1038/s42256-019-0048-x

Ryo, M., Iwasaki, Y., Yoshimura, C., & V, O. C. S. (2015). Evaluation of Spatial Pattern of Altered Flow Regimes on a River Network Using a Distributed Hydrological Model. *PLOS ONE*, *10*(7), e0133833. https://doi.org/10.1371/journal.pone.0133833

911 Sanborn, S. C., & Bledsoe, B. P. (2006). Predicting streamflow regime metrics for ungauged
912 streamsin Colorado, Washington, and Oregon. *Journal of Hydrology*, *325*(1), 241–261.
913 https://doi.org/10.1016/j.jhydrol.2005.10.018
914 Sang, Y.-F. (2013). A review on the applications of wavelet transform in hydrology time series
915 analysis. *Atmospheric Research*, *122*(Supplement C), 8–15.
916 https://doi.org/10.1016/j.atmosres.2012.11.003
917 Savenije, H. H. G. (2018). HESS Opinions: Linking Darcy's equation to the linear reservoir.
918 *Hydrology and Earth System Sciences*, *22*(3), 1911–1916. https://doi.org/10.5194/hess-
919 22-1911-2018
920 Schneider, C., Laizé, C. L. R., Acreman, M. C., & Flörke, M. (2013). How will climate change
921 modify river flow regimes in Europe? *Hydrology and Earth System Sciences*, *17*(1), 325–
922 339. https://doi.org/10.5194/hess-17-325-2013
923 Sivapalan, M. (2006). Pattern, Process and Function: Elements of a Unified Theory of
924 Hydrology at the Catchment Scale. In *Encyclopedia of Hydrological Sciences*. John
925 Wiley & Sons, Ltd. https://doi.org/10.1002/0470848944.hsa012
926 Smith, L. C., Turcotte, D. L., & Isacks, B. L. (1998). Stream flow characterization and feature
927 detection using a discrete wavelet transform. *Hydrological Processes*, *12*(2), 233–249.
928 https://doi.org/10.1002/(SICI)1099-1085(199802)12:2<233::AID-HYP573>3.0.CO;2-3
929 Sposito, G. (2017). Understanding the Budyko Equation. *Water*, *9*(4), 236.
930 https://doi.org/10.3390/w9040236
931 Tague, C., & Grant, G. E. (2004). A geological framework for interpreting the low-flow regimes
932 of Cascade streams, Willamette River Basin, Oregon. *Water Resources Research*, *40*(4).
933 https://doi.org/10.1029/2003WR002629

Tank, S. E., Vonk, J. E., Walvoord, M. A., McClelland, J. W., Laurion, I., & Abbott, B. W. (2020). Landscape matters: Predicting the biogeochemical effects of permafrost thaw on aquatic networks with a state factor approach. *Permafrost and Periglacial Processes*, *31*(3), 358–370. https://doi.org/10.1002/ppp.2057

Teixeira, H., Lillebø, A. I., Culhane, F., Robinson, L., Trauner, D., Borgwardt, F., et al. (2019). Linking biodiversity to ecosystem services supply: Patterns across aquatic ecosystems. *Science of The Total Environment*, *657*, 517–534. https://doi.org/10.1016/j.scitotenv.2018.11.440

Tetzlaff, D., McDonnell, J., Uhlenbrook, S., McGuire, K., Bogaart, P., Naef, F., et al. (2008). Conceptualizing catchment processes: Simply too complex? *Hydrological Processes 22 (2008) 11*, *22*. https://doi.org/10.1002/hyp.7069

Torrence, C., & Compo, G. P. (1998). A Practical Guide to Wavelet Analysis. *Bulletin of the American Meteorological Society*, *79*(1), 61–78. https://doi.org/10.1175/1520-0477(1998)079<0061:APGTWA>2.0.CO;2

Tucker, G. E., & Hancock, G. R. (2010). Modelling landscape evolution. *Earth Surface Processes and Landforms*, *35*(1), 28–50. https://doi.org/10.1002/esp.1952

Van Loon, A. F., Gleeson, T., Clark, J., Van Dijk, A. I. J. M., Stahl, K., Hannaford, J., et al. (2016). Drought in the Anthropocene. *Nature Geoscience*, *9*(2), 89–91. https://doi.org/10.1038/ngeo2646

Virtanen, P., Gommers, R., Oliphant, T. E., Haberland, M., Reddy, T., Cournapeau, D., et al. (2020). SciPy 1.0: fundamental algorithms for scientific computing in Python. *Nature Methods*, *17*(3), 261–272. https://doi.org/10.1038/s41592-019-0686-2

Vörösmarty, C. J., McIntyre, P. B., Gessner, M. O., Dudgeon, D., Prusevich, A., Green, P., et al. (2010). Global threats to human water security and river biodiversity. *Nature*, *467*(7315), 555–561. https://doi.org/10.1038/nature09440

Wenger, S. J., Isaak, D. J., Luce, C. H., Neville, H. M., Fausch, K. D., Dunham, J. B., et al. (2011). Flow regime, temperature, and biotic interactions drive differential declines of trout species under climate change. *Proceedings of the National Academy of Sciences*, *108*(34), 14175–14180. https://doi.org/10.1073/pnas.1103097108

White, M. A., Schmidt, J. C., & Topping, D. J. (2005). Application of wavelet analysis for monitoring the hydrologic effects of dam operation: Glen Canyon Dam and the Colorado River at Lees Ferry, Arizona. *River Research and Applications*, *21*(5), 551–565. https://doi.org/10.1002/rra.827

Wolff, J. G. (2019). Information Compression as a Unifying Principle in Human Learning, Perception, and Cognition. *Complexity*, *2019*, e1879746. https://doi.org/10.1155/2019/1879746

Wu, S., Zhao, J., Wang, H., & Sivapalan, M. (2021). Regional Patterns and Physical Controls of Streamflow Generation Across the Conterminous United States. *Water Resources Research*, *57*(6), e2020WR028086. https://doi.org/10.1029/2020WR028086

Xenopoulos, M. A., & Lodge, D. M. (2006). Going with the Flow: Using Species–Discharge Relationships to Forecast Losses in Fish Biodiversity. *Ecology*, *87*(8), 1907–1914. https://doi.org/10.1890/0012-9658(2006)87[1907:GWTFUS]2.0.CO;2

Zammit-Mangion, A., & Cressie, N. (2017). FRK: An R Package for Spatial and Spatio-Temporal Prediction with Large Datasets.

978 Zarnetske, J. P., Bouda, M., Abbott, B. W., Saiers, J., & Raymond, P. A. (2018). Generality of
979 Hydrologic Transport Limitation of Watershed Organic Carbon Flux Across Ecoregions
980 of the United States. *Geophysical Research Letters*, *45*(21), 11,702-11,711.
981 https://doi.org/10.1029/2018GL080005
982 Zhou, G., Wei, X., Chen, X., Zhou, P., Liu, X., Xiao, Y., et al. (2015). Global pattern for the
983 effect of climate and land cover on water yield. *Nature Communications*, *6*(1), 5918.
984 https://doi.org/10.1038/ncomms6918
985 Zipper, S. C., Jaramillo, F., Wang-Erlandsson, L., Cornell, S. E., Gleeson, T., Porkka, M., et al.
986 (2020). Integrating the Water Planetary Boundary With Water Management From Local
987 to Global Scales. *Earth's Future*, *8*(2), e2019EF001377.
988 https://doi.org/10.1029/2019EF001377

989
990
991

Figure 1.

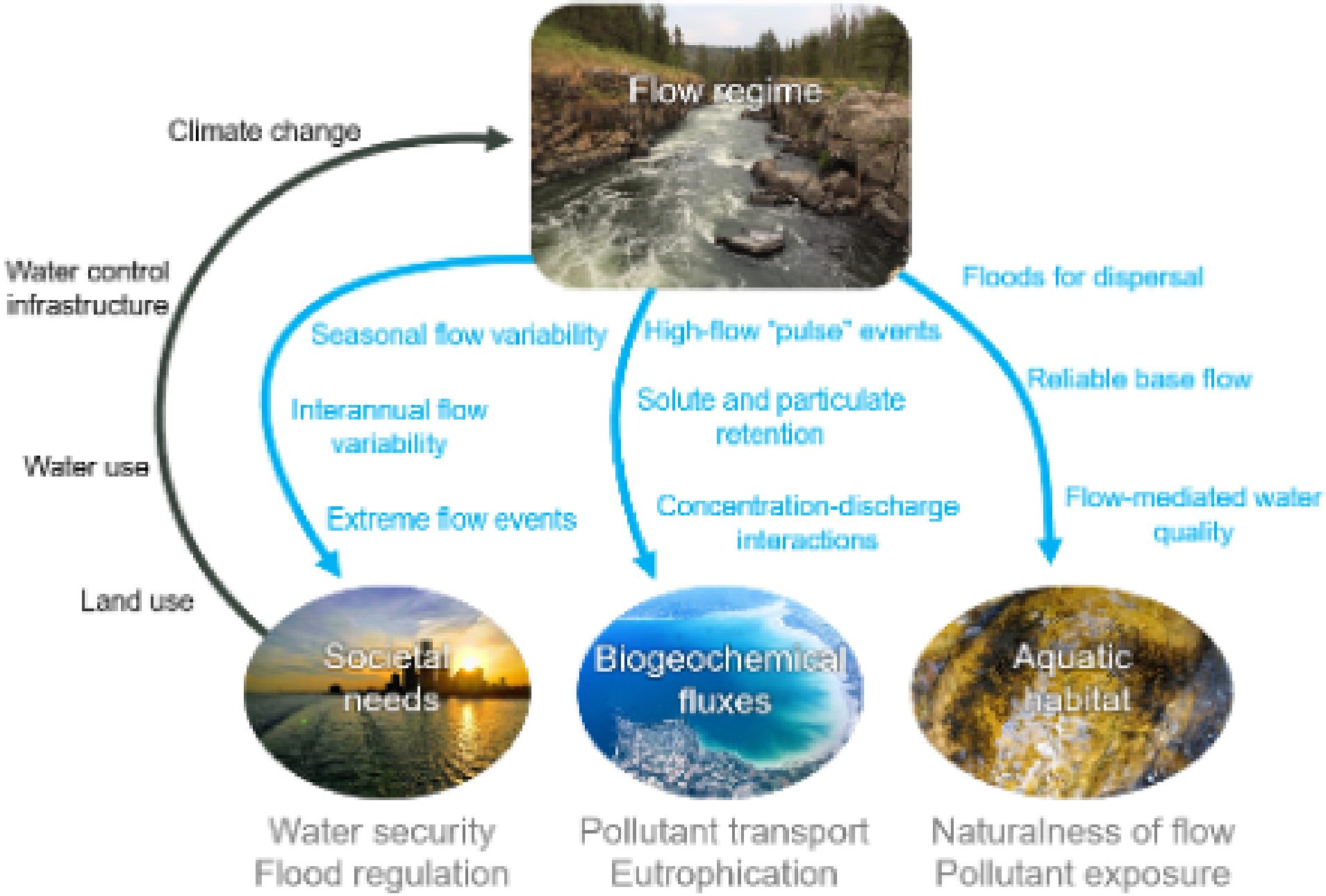
Flow regime
Climate change
Water control infrastructure
Water use
Land use
Seasonal flow variability
Interannual flow variability
Extreme flow events
High-flow "pulse" events
Solute and particulate retention
Concentration-discharge interactions
Floods for dispersal
Reliable base flow
Flow-mediated water quality
Societal needs
Biogeochemical fluxes
Aquatic habitat
Water security
Flood regulation
Pollutant transport
Eutrophication
Naturalness of flow
Pollutant exposure

Figure 2.

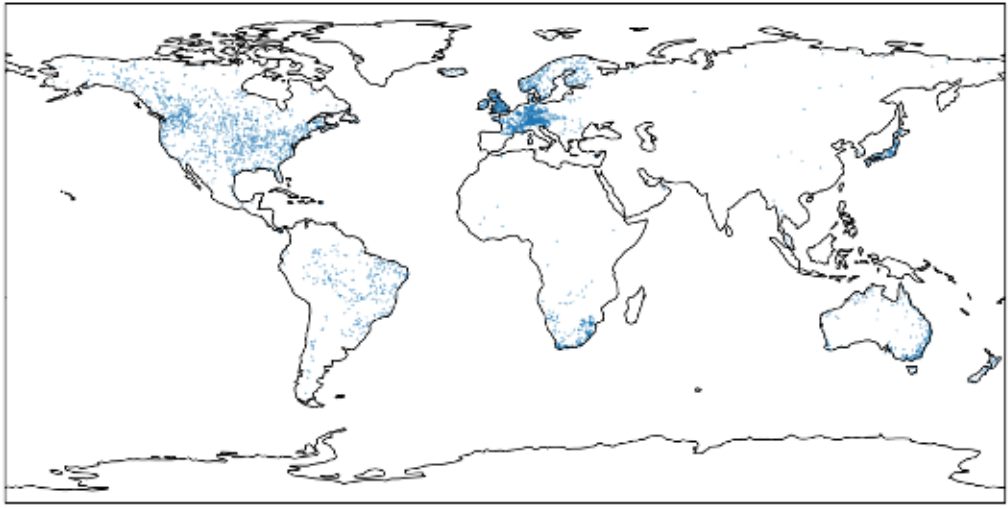
Distribution of Study Catchments

Figure 3.

a) Phase (horizontal shift)

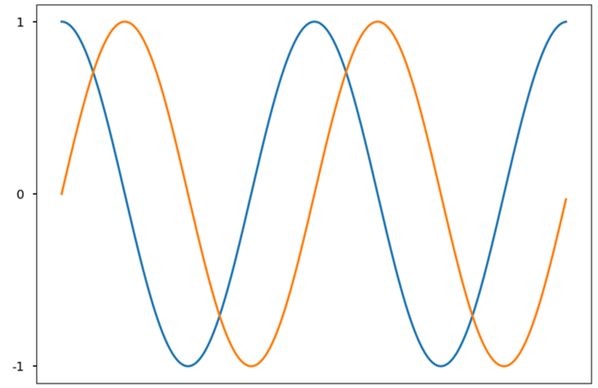

b) Amplitude

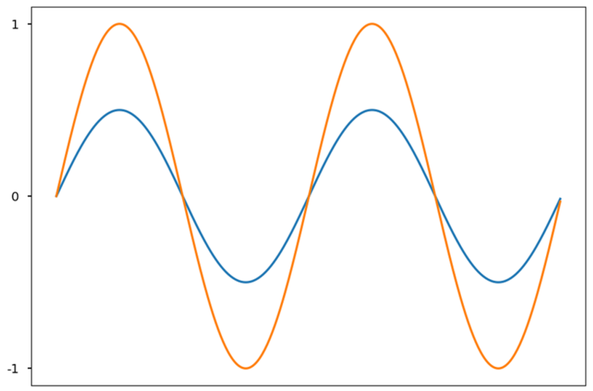

c) Vertical shift

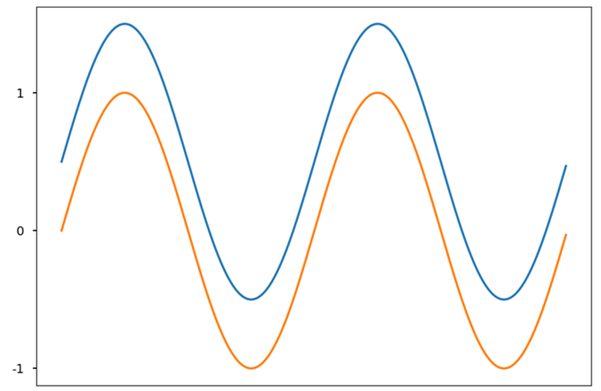

d) Frequency

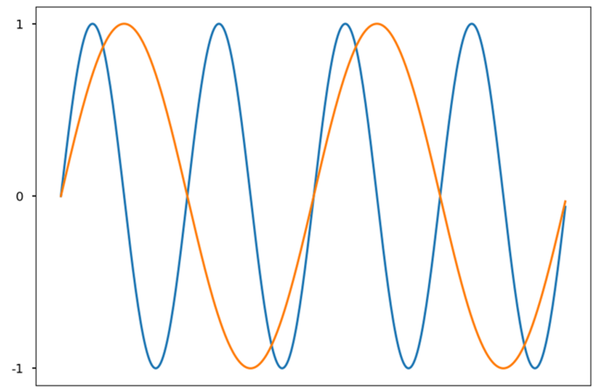

e) Waveform

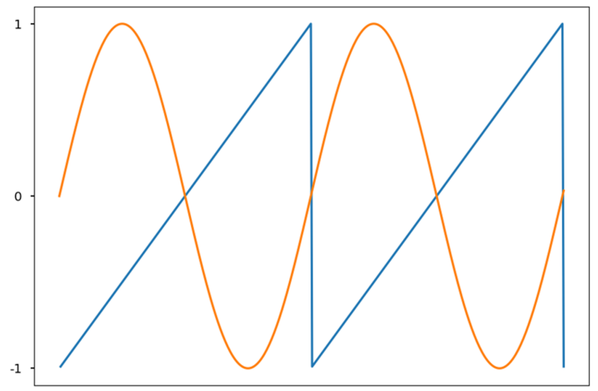

Can answer questions about these qualities

Frequency decomposition

f)

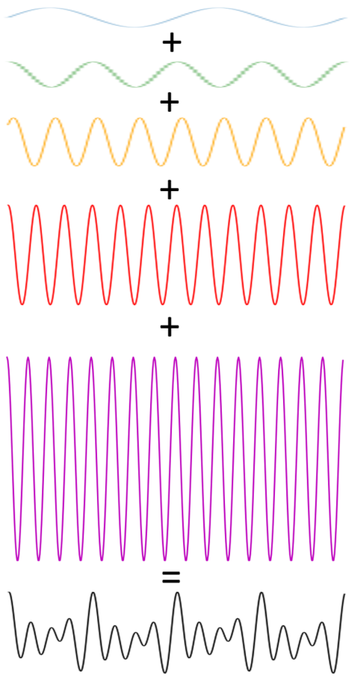

g)

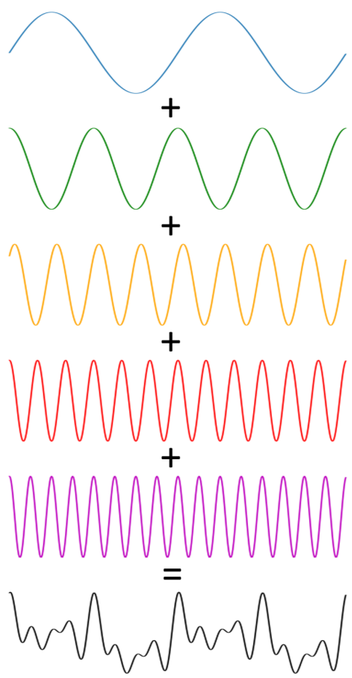

h)

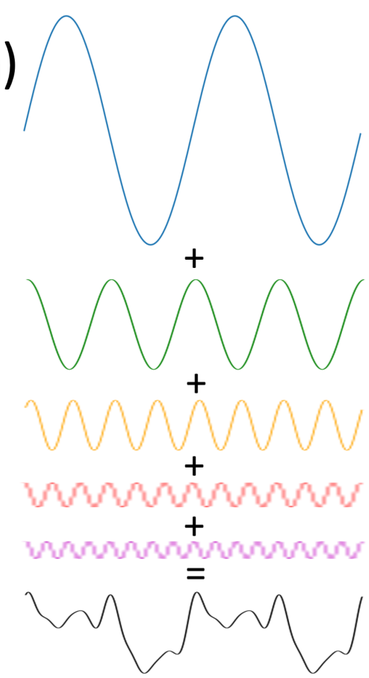

Amplitude is similar to spectral power

Figure 4.

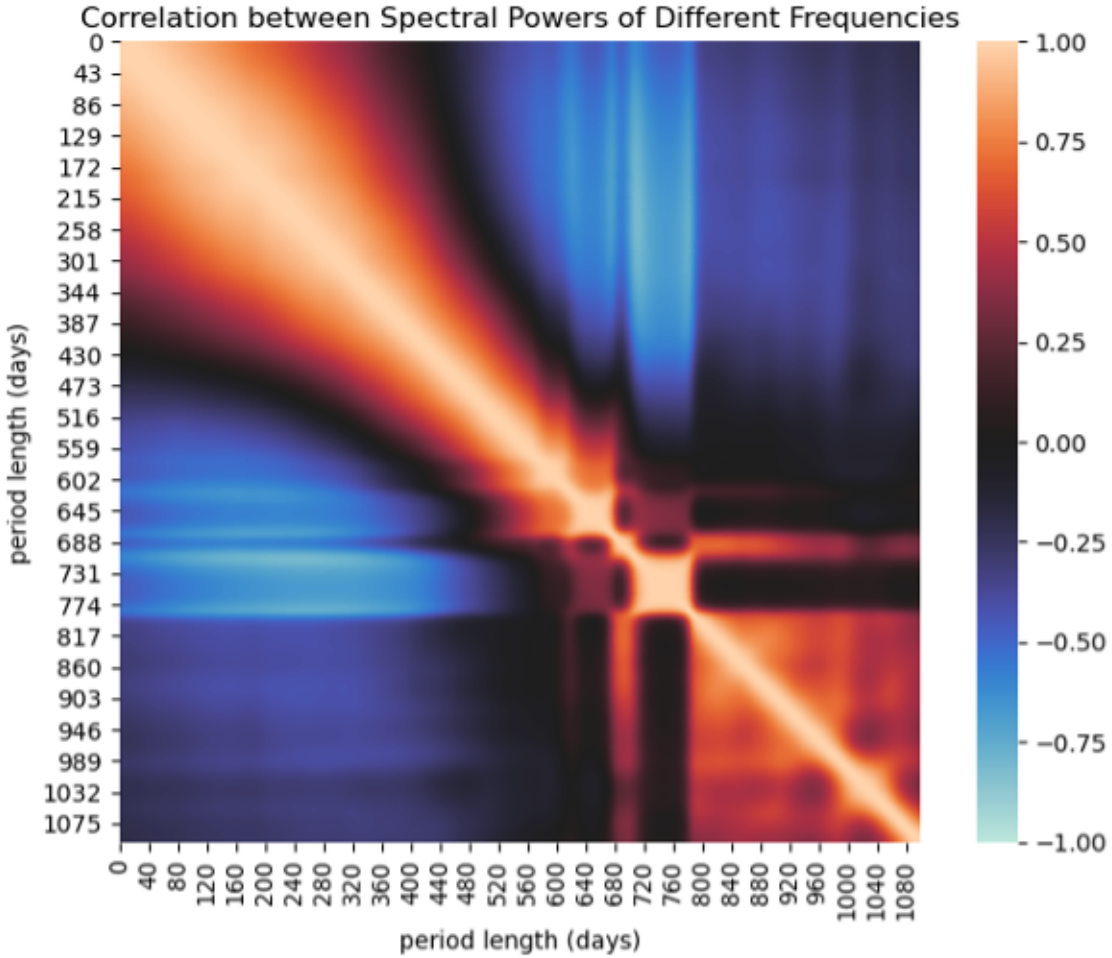
Correlation between Spectral Powers of Different Frequencies
period length (days)
0
43
86
129
172
215
258
301
344
387
430
473
516
559
602
645
688
731
774
817
860
903
946
989
1032
1075
0
40
80
120
160
200
240
280
320
360
400
440
480
520
560
600
640
680
720
760
800
840
880
920
960
1000
1040
1080
period length (days)
1.00
0.75
0.50
0.25
0.00
−0.25
−0.50
−0.75
−1.00

Figure 5.

Frequency Domain

Time Domain

Spectral power concentrated on short period lengths

Spectral power concentrated on long period lengths

Increasing flashiness

Increasingly-sustained annual flooding

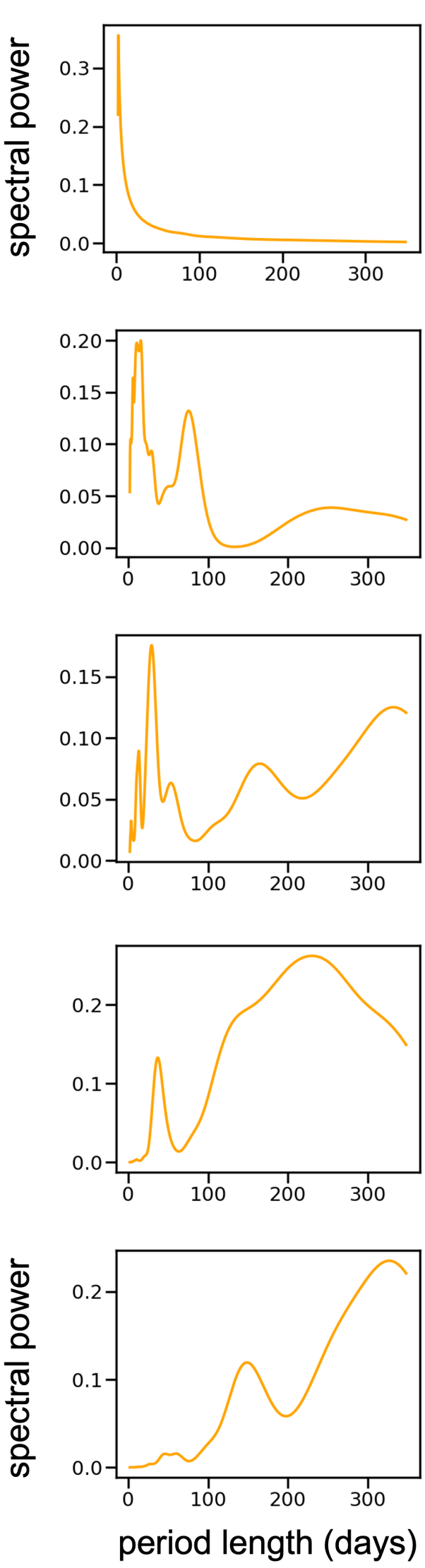

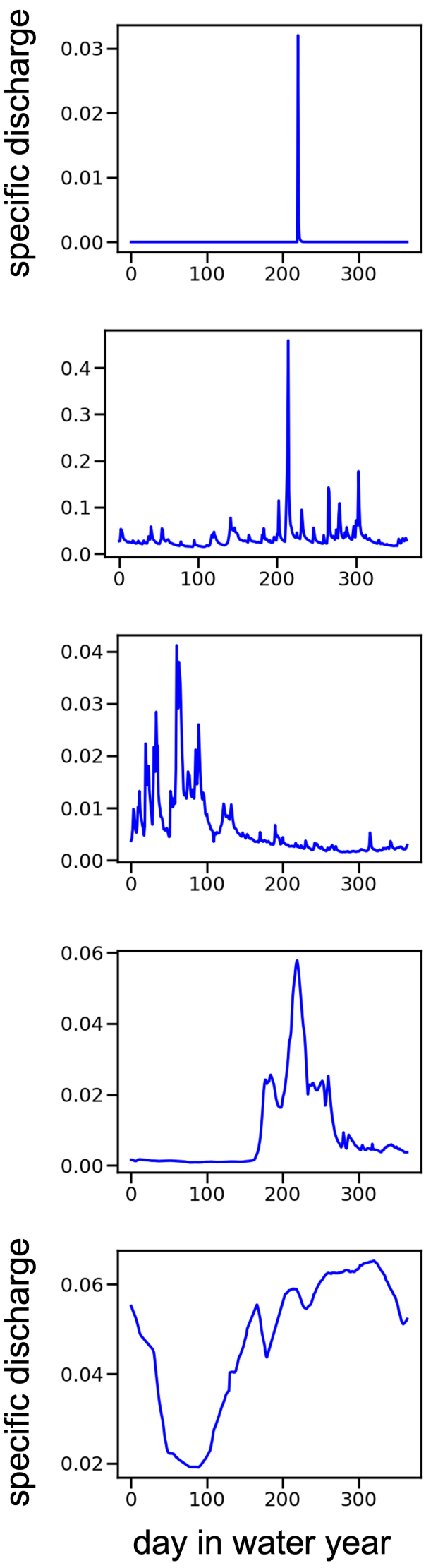

Figure 6.

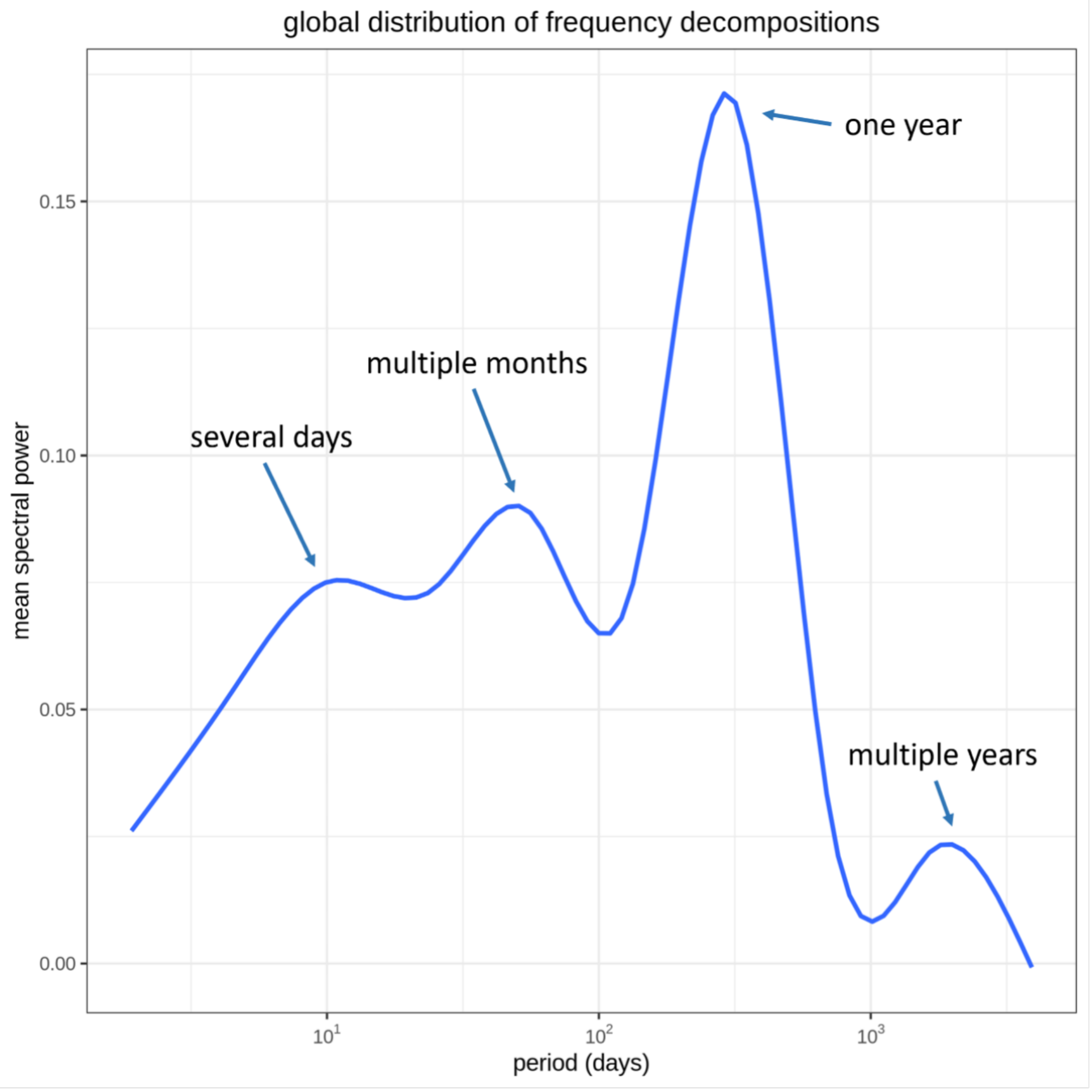
global distribution of frequency decompositions
one year
multiple months
several days
multiple years
mean spectral power
0.15
0.10
0.05
0.00
10^1
10^2
10^3
period (days)

Figure 7.

a)

b)

c)

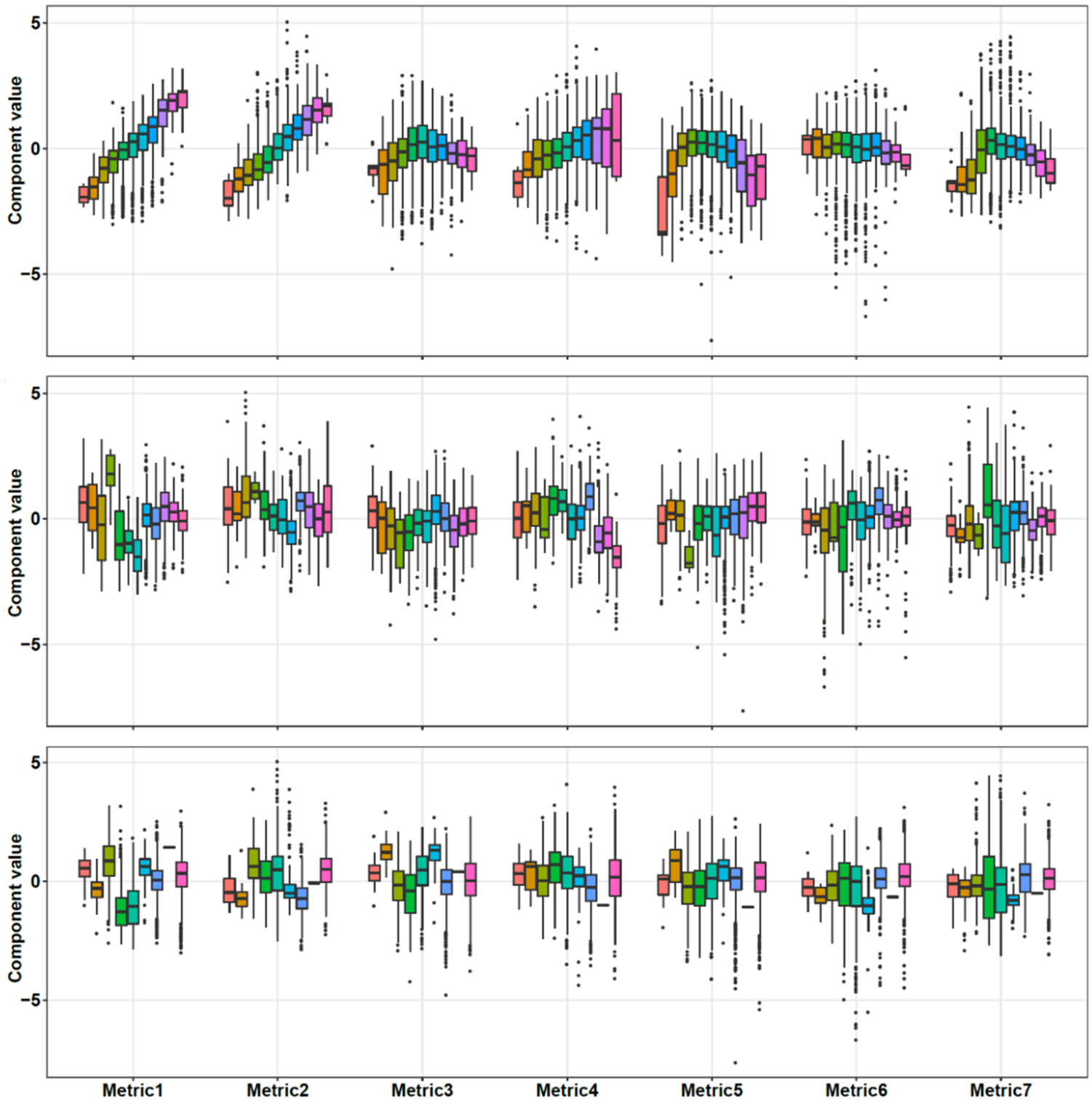

Stream Order

1
2
3
4
5
6
7
8
9
10
11

Biome

Tropical and Subtropical Moist Broadleaf Forests
Tropical and Subtropical Dry Broadleaf Forests
Tropical and subtropical grasslands, savannas, and shrublands
Flooded Grasslands and Savannas
Deserts and Xeric Shrublands
Montane Grasslands and Shrublands
Mediterranean Forests, Woodlands, and Scrub
Temperate Broadleaf and Mixed Forests
Temperate Grasslands, Savannas, and Shrublands
Boreal Forests/Taiga
Temperate Coniferous Forests
Tundra

Continental region

Southern Asia
Central America
South America
Africa and Madagascar
Australia and Pacific
Northern Asia
Europe and Middle East
North America

Figure 8.

Metric 1
Metric 2
Metric 3
Metric 4
Metric 5
Metric 6
Metric 7
5
0
−5
−10
0
10
20
30
0
200
400
600
10
1000
100,000
0
25
50
75
100
Mean temperature (C)
Mean precipitation (mm)
Catchment size (km^2)
Forest (%)
Human (%)
Stream order class
1
2
3
4

Figure 9.

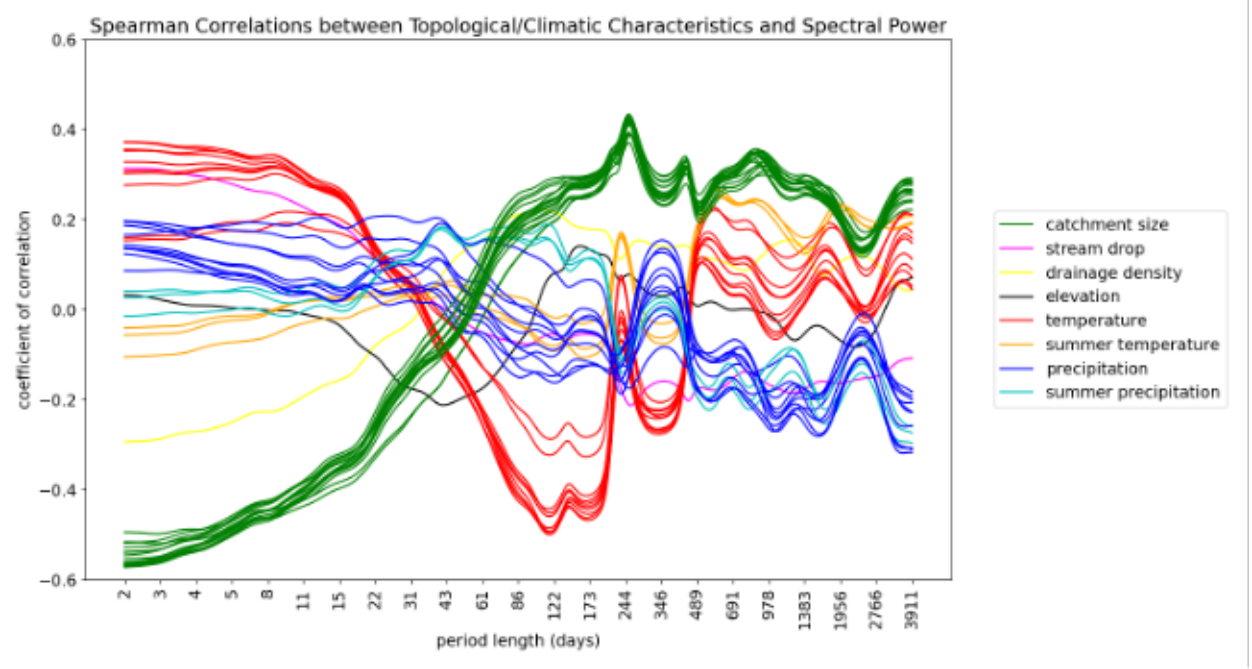
Spearman Correlations between Topological/Climatic Characteristics and Spectral Power
coefficient of correlation
0.6
0.4
0.2
0.0
−0.2
−0.4
−0.6
2
3
4
5
8
11
15
22
31
43
61
86
122
173
244
346
489
691
978
1383
1956
2766
3911
period length (days)
catchment size
stream drop
drainage density
elevation
temperature
summer temperature
precipitation
summer precipitation

Figure 10.

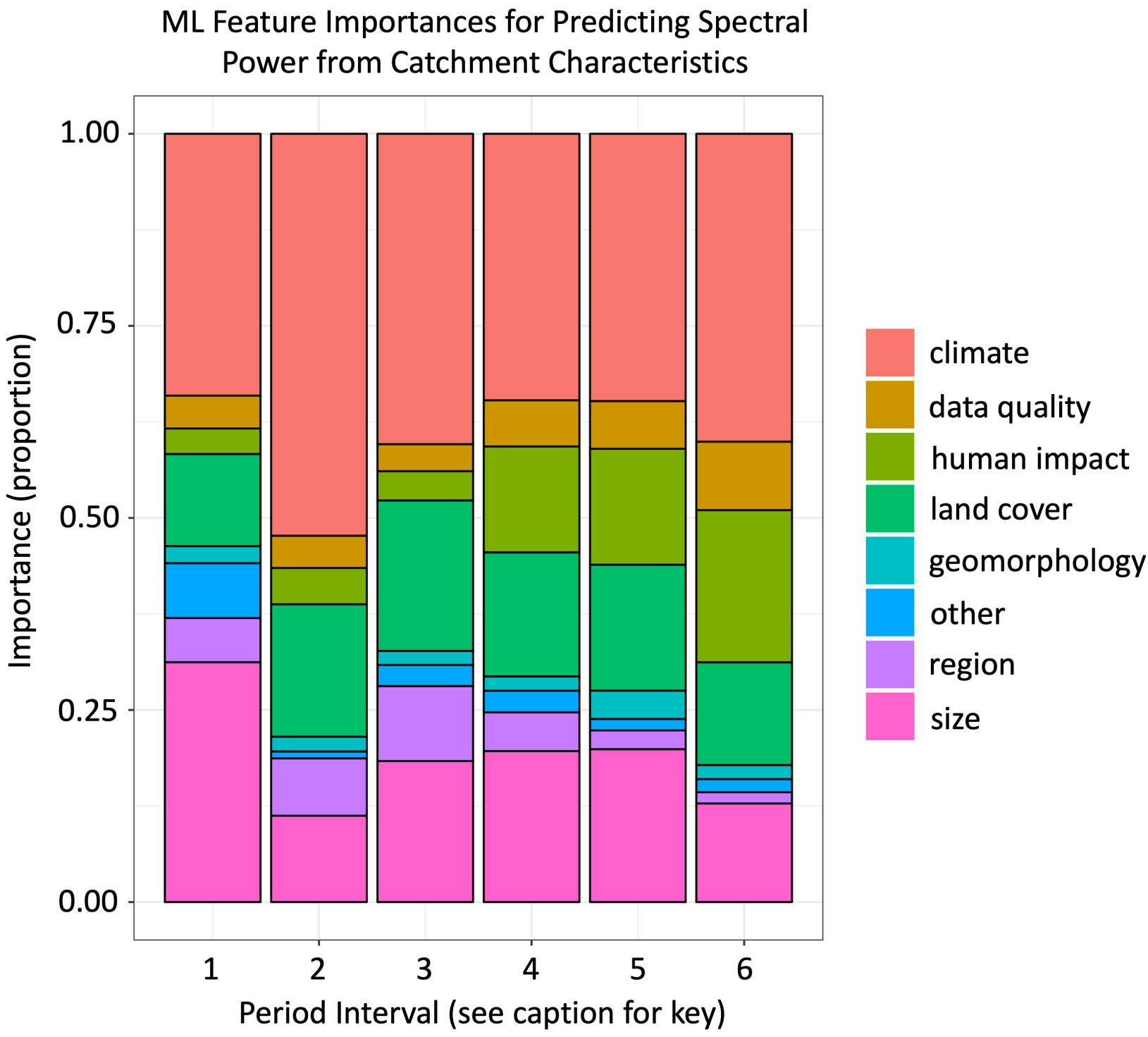
ML Feature Importances for Predicting Spectral Power from Catchment Characteristics
Importance (proportion)
1.00
0.75
0.50
0.25
0.00
1
2
3
4
5
6
Period Interval (see caption for key)
climate
data quality
human impact
land cover
geomorphology
other
region
size